Linkage Isomers and Their Enantiomeric Siblings as CPL-TADF Emitters: Modulating Chirality and Enhancing Dissymmetry Factor Through N- and O-Linked Carbazoles

Diksha Thakur[a⊥], Biswaranjan Sahu[a⊥], Wijak Yospanya,[b] Reiko Oda,[b,c] Sivakumar Vaidyanathan[a]*

Department of Chemistry, Indian Institute of Technology, Hyderabad, Sangareddy 502285, Telangana, India.

[b]Advanced Institute for Materials Research (AIMR), Tohoku University, 2-1-1 Katahira, Aoba, Sendai, Miyagi, Japan

[c]University of Bordeaux, CNRS, Bordeaux INP, CBMN, UMR 5248, F-33600 Pessac, France

General Information

All commercial reagents, purchased from BLD, Alpha Aesar, TCI, and Merck, were used without further purification. ^{1}H NMR (400 MHz) and ^{13}C NMR (100 MHz), were recorded on BRUKER ASCEND 400 MHz. HRMS spectra were recorded using an Agilent UHD Accurate-Mass Q-TOF LC/MS. UV-visible spectra were recorded on Jasco V730 (Model name V-730; Serial No. C216361798; Data interval: 1 nm; Bandwidth: 1.0 nm; Response: 0.96 sec; Scan mode: Continuous; Scan speed: 400 nm/min). Circular dichroism (CD) spectra were recorded on Jasco J-815 CD Spectrometer (Sensitivity: Standard; Bandwidth: 10.00 nm; Start mode: Immediately; Scanning speed: 200 nm/min). Photoluminescence spectra in solution were recorded on JASCOFP-8350 spectrofluorometer (Ex bandwidth: 5 nm; Em bandwidth: 10 nm; Response: 1 sec; Sensitivity: Medium; Measurement range: 340 - 640 nm; Data interval: 1 nm; Ex wavelength: 326.0 nm; Scan speed: 500 nm/min). Thin film PL spectra were measured in Horiba Fluoromax-4. TCSPC experiments were performed on Horiba Fluoromax-4 (370 nm excitation LASER). The circularly polarized luminescence (CPL) measurements were performed on CPL-300 (serial number: H005361854; Pathlength: 2 mm; Scan Speed: 200 nm/min). Density functional theory calculations were performed with the Gaussian 16 using B3LYP 6-31 G(d).[1]

A specific response is generated upon interaction of circularly polarized light with the chiral molecules, which is opposite in sign for both enantiomers. This response can be characterized by circular dichroism spectroscopy. The extent of circular polarization can be defined by the absorption dissymmetry factor (g_{abs}) and luminescence dissymmetry factor (g_{lum}). The absorption dissymmetry factor (g_{abs}) can be measured by circular dichroism (CD) spectroscopy and is defined by the following equation:[2]

$$g_{abs} = 2(\varepsilon_L - \varepsilon_R)/ (\varepsilon_L + \varepsilon_R)$$

where; ε_L = extinction coefficient for left-handed circularly polarized light; ε_R = extinction coefficient for right-handed circularly polarized light

In CPL spectroscopy, the emission intensity difference between L- and R-CPL is given by following equation[2,3]

$$\Delta I = I_L - I_R$$

$$g_{lum} = 2(I_L - I_R)/(I_L + I_R)$$

where; I_L = emission intensity of left-handed CPL; I_R = emission intensity of right-handed CPL. The above equation mentions that the dissymmetry factor varies from +2 to -2. A maximum value of $g_{lum} = \pm 2$ indicates absolute left- or right-handed circular polarization of emitted light, whereas $g_{lum} = 0$ indicates no circular polarization.[3,4]

Many molecular design approaches are available which help engineer the small $\Delta E_{ST.}$ The separation of the HOMO and LUMO leads to this small energy gap in the organic molecule. The rate of reverse intersystem crossing (k_{RISC}) is connected to the ΔE_{ST} and the temperature by the following equation, indicating that the small ΔE_{ST} increases the k_{RISC}.[5]

$$k_{RISC} \propto \exp\left(-\frac{\Delta E_{ST}}{k_B T}\right) \quad \ldots\ldots\ldots 1$$

Using strong donor and acceptor units, along with introducing steric hindrance and twisted donor-acceptor geometry, can effectively achieve the separation of the HOMO and LUMO.[5]

Synthetic procedures

1. Synthetic procedure for RBN-DCNB/SBN-DCNB:

RBN-DCNB/SBN-DCNB was synthesized according to the literature procedure.[6] To a 100 mL flask, DMF was added to dissolve **RBN/SBN** (1 equivalent) and tetrafluorodicyanobenzene (1 equivalent). Potassium carbonate (2.2 equivalents) was added, and the reaction mixture was stirred for 12h at room temperature under nitrogen. After completion of the reaction, monitored by thin-layer chromatography, ice water was added. The organic layer was extracted with dichloromethane. The solvent was then removed under vacuum, and the solid was purified by flash column chromatography.

2. Synthetic procedure for CZ4BTXY

CZ4BTXY was synthesized according to the procedure in the literature.[7] 9H-carbazol-4-ol (1 eq), potassium carbonate (2 eq), tetrabutyl ammonium bromide (0.01 eq), and ethyl acetate were added to a round-bottom flask equipped with a magnetic stir bar. The reaction was first run at room temperature for 1 h. Then, bromobutane (3 eq) was added to the solution and heated at 75°C for 24 h. After the reaction was finished (checked with TLC), the mixture was extracted with water and ethyl acetate. After drying over anhydrous Na_2SO_4, ethyl acetate was removed on a rotary evaporator. The crude product was purified by column chromatography.

3. Synthetic procedure for R-CZ4BTXY/S-CZ4BTXY;

The above-mentioned compounds were synthesized according to the procedure in the literature.[2]

To a 100 mL flask, DMF was added to dissolve **RBN-DCNB/SBN-DCNB** (1 equivalent) and CZ4BTXY (2 equivalent). Potassium carbonate (5 equivalent) was added and the reaction mixture was stirred for 12h at room temperature under nitrogen. After completion of the reaction monitored by thin-layer chromatography, ice water, and dichloromethane were added. The organic layer was extracted with dichloromethane. The solvent was then removed under vacuum and the solid was purified by flash column chromatography.

4. Synthetic procedure for R-CZ4OH/S-CZ4OH

To a 100 mL flask, DMF was added to dissolve **RBN-DCNB/SBN-DCNB** (1 equivalent) and 4-hydroxy carbazole (2 equivalent). Potassium carbonate (5 equivalent) was added and the reaction mixture was stirred for 12h at room temperature under nitrogen. After completion of the reaction monitored by thin-layer chromatography, ice water, and dichloromethane were added. The organic layer was extracted with dichloromethane. The solvent was then removed under vacuum and the solid was purified by flash column chromatography.

5. Synthetic procedure for R-NBTOCZ/S-NBTOCZ;

To a 100 mL flask, DMF was added to dissolve **R-CZ4OH/S-CZ4OH** (1 equivalent) and followed by addition of NaH (3 equivalent). The reaction was made to run at RT for one hour followed by addition of bromobutane (4 equivalent). The reaction mixture was stirred for 6h at 70 °C. After completion of the reaction monitored by thin-layer chromatography, ice water, and dichloromethane were added. The organic layer was extracted with dichloromethane. The solvent was then removed under vacuum and the solid was purified by flash column chromatography.

Table S1. CIE (1931) color coordinates for the developed isomers in the THF-water experiment at different water fractions.

R-CZ4BTXY			R-NBTOCZ		
Water Fraction (% fw)	x	y	Water Fraction (% fw)	x	y
0	0.19752	0.15931	0	0.17466	0.10787
10	0.16741	0.08202	10	0.15577	0.04792
20	0.16646	0.08271	20	0.15729	0.05849
30	0.16611	0.08325	30	0.15557	0.05064
40	0.17059	0.09927	40	0.15685	0.05856
50	0.16362	0.07635	50	0.15559	0.05396
60	0.17036	0.09479	60	0.15468	0.05056
70	0.27786	0.3581	70	0.18844	0.14892
80	0.32694	0.51272	80	0.25136	0.34739
90	0.33916	0.58857	90	0.27762	0.54446
100	0.34735	0.61022	100	0.27051	0.57664

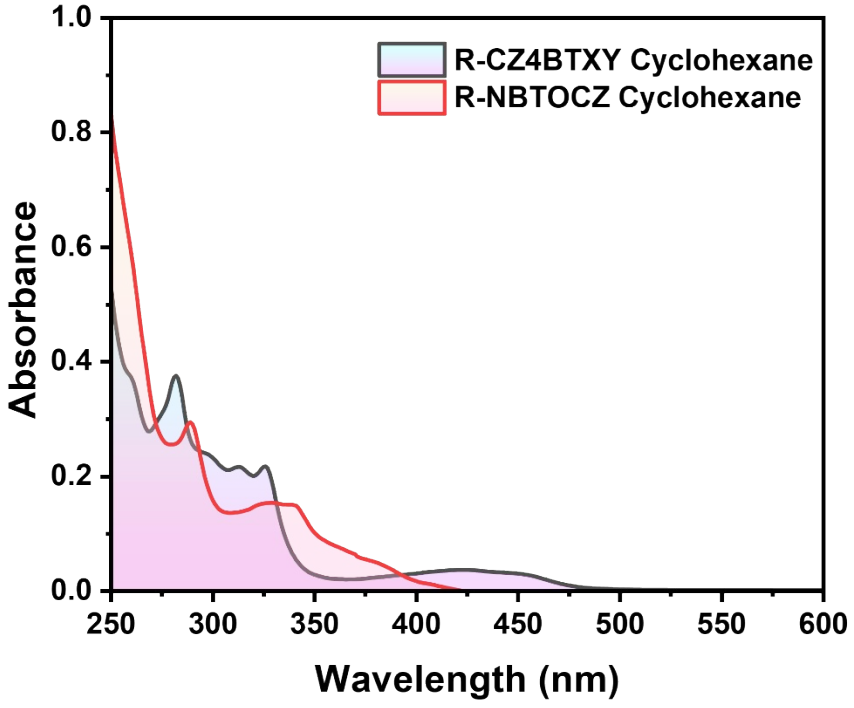

Fig. S1. UV-vis absorption spectra of R-CZ4BTXY and R-NBTOCZ in cyclohexane (10 micromolar).

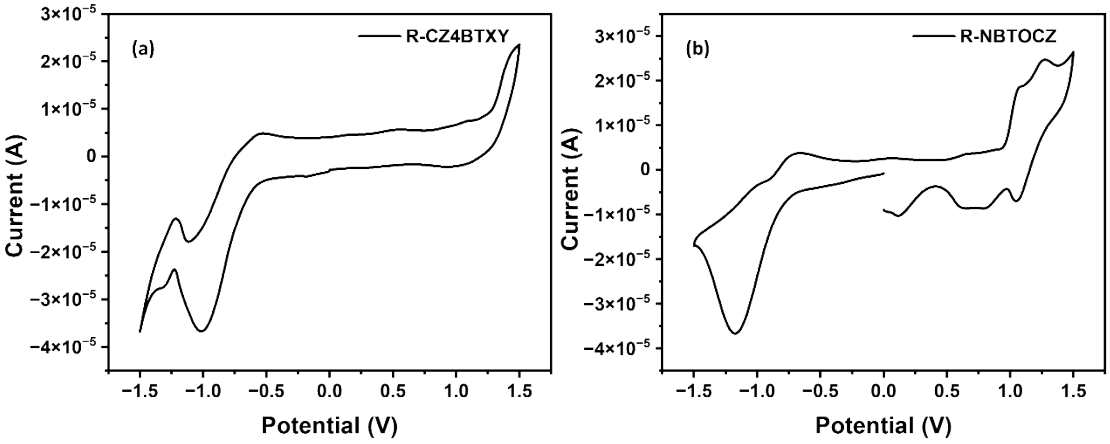

Fig. S2. Cyclic voltammetry plots of the synthesized compounds (a) R-CZ4BTXY and (b) R-NBTOCZ.

Table S2. Luminescence dissymmetry factor of some previously reported chiral emitters.

Compound	Luminescence dissymmetry factor	Reference	Reference
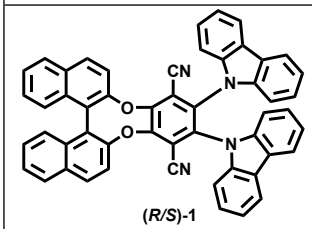 (*R/S*)-1	$\lvert g_{lum}\rvert = 1.3\times10^{-3}$	J. Am. Chem. Soc. 2016, 138, 3990−3993	6
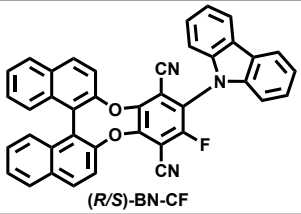 (*R/S*)-BN-CF	g_{lum} = -1.0×10^{-3} /1.2×10^{-3} (*R/S*)	Adv. Funct. Mater. 2018, 28, 1800051	8
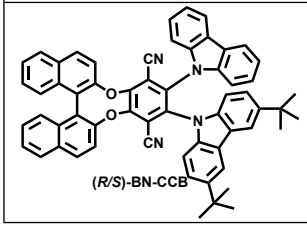 (*R/S*)-BN-CCB	g_{lum} = -1.2×10^{-3} /1.1×10^{-3} (*R/S*)	Adv. Funct. Mater. 2018, 28, 1800051	8

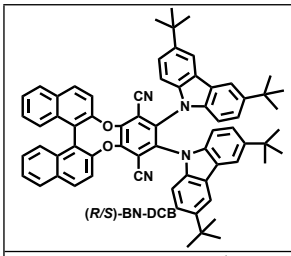 (*R/S*)-BN-DCB	g_{lum} = -9 ×10^{-4}/7 ×10^{-4} (*R/S*)	Adv. Funct. Mater. 2018, 28, 1800051	[8]
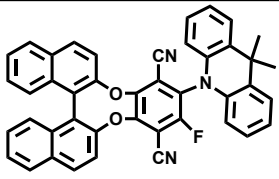 (*R/S*)-BN-AF	g_{lum} = -7×10^{-4}/5 ×10^{-4} (*R/S*)	Adv. Funct. Mater. 2018, 28, 1800051	[8]
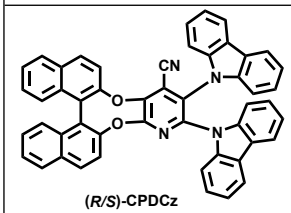 (*R/S*)-CPDCz	g_{PL}= 3.4×10^{-4}/-3.0×10^{-4} (*R/S*)	J. Mater. Chem. C, 2019, 7, 14511--14516	[9]
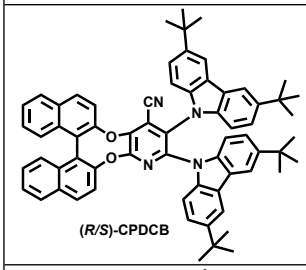 (*R/S*)-CPDCB	g_{PL}=3.2×10^{-4}/-2.1×10^{-4} (*R/S*)	J. Mater. Chem. C, 2019, 7, 14511--14516	[9]
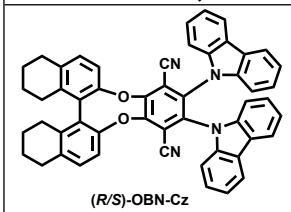 (*R/S*)-OBN-Cz	g_{PL}= -4.6×10^{-3}/5.6×10^{-3} (*R/S*)	Adv. Mater. 2019, 31, 1900524	[10]
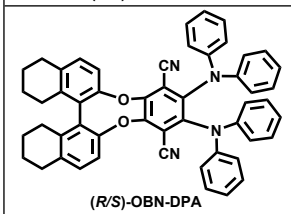 (*R/S*)-OBN-DPA	g_{PL}= 1.88×10^{-3}/ -1.75×10^{-3} (*R/S*)	J. Mater. Chem. C, 2019, 7, 7045--7052	[11]
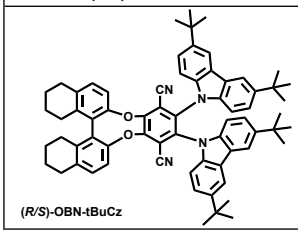 (*R/S*)-OBN-tBuCz	g_{PL}= -6.5×10^{-4}/8.6×10^{-4} (*R/S*)	Acta Chim. Sinica 2021, 79, 1401—1408	[12]
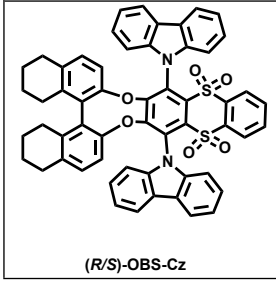 (*R/S*)-OBS-Cz	$\|g_{PL}\|$ = 7×10^{-4}	ACS Appl. Mater. Interfaces 2021, 13, 56413−56419	[13]

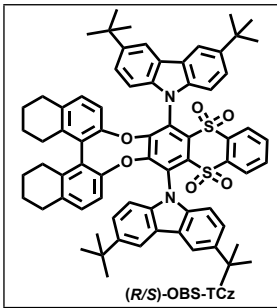 (*R*/*S*)-OBS-TCz	$\lvert g_{PL}\rvert$ = 3.9×10^{-4}	ACS Appl. Mater. Interfaces 2021, 13, 56413−56419	[13]

NMR Spectra

1. SBN-DCNB: ^{1}H NMR (400 MHz, $CDCl_3$) δ 8.08 (d, *J* = 8.9 Hz, 2H), 8.00 (d, *J* = 8.2 Hz, 2H), 7.59 – 7.40 (m, 8H).

^{13}C NMR (100 MHz, $CDCl_3$) δ 149.11, 148.43, 147.32, 147.29, 145.86, 145.65, 132.45, 132.05, 131.92, 128.70, 127.77, 126.80, 126.74, 124.97, 120.20, 108.98.

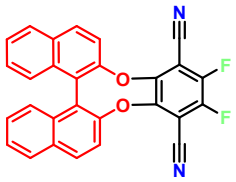

SBN-DCNB

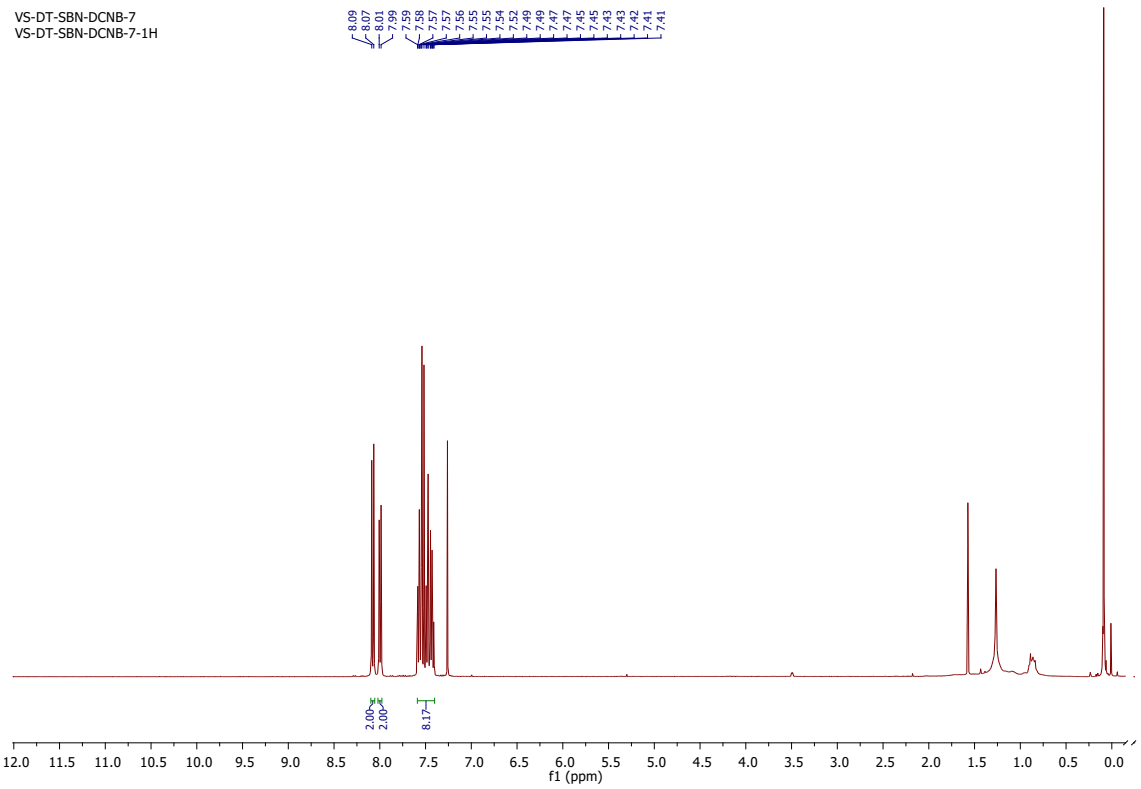

Fig. S3. ^{1}H NMR of SBN-DCNB. (peaks at 0.9 and 1.3 correspond to grease; peak at 1.6 corresponds to moisture in $CDCl_3$)

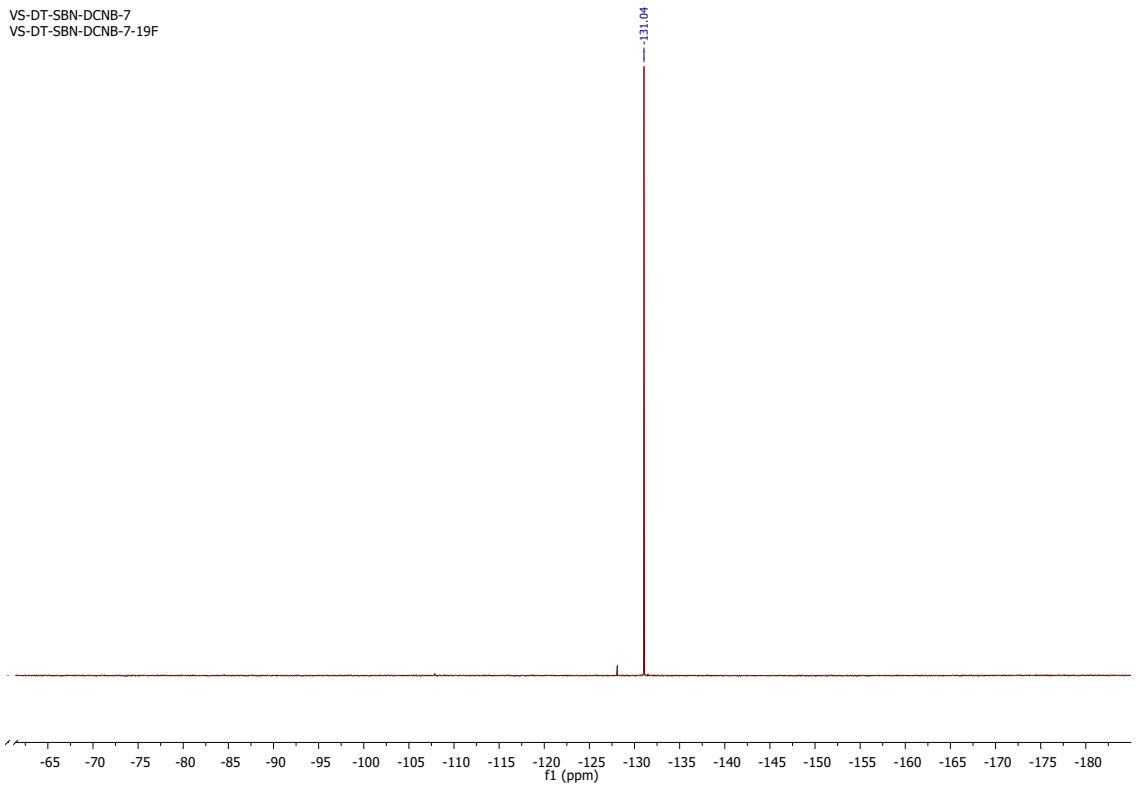

Fig. S4. ^{19}F NMR of SBN-DCNB.

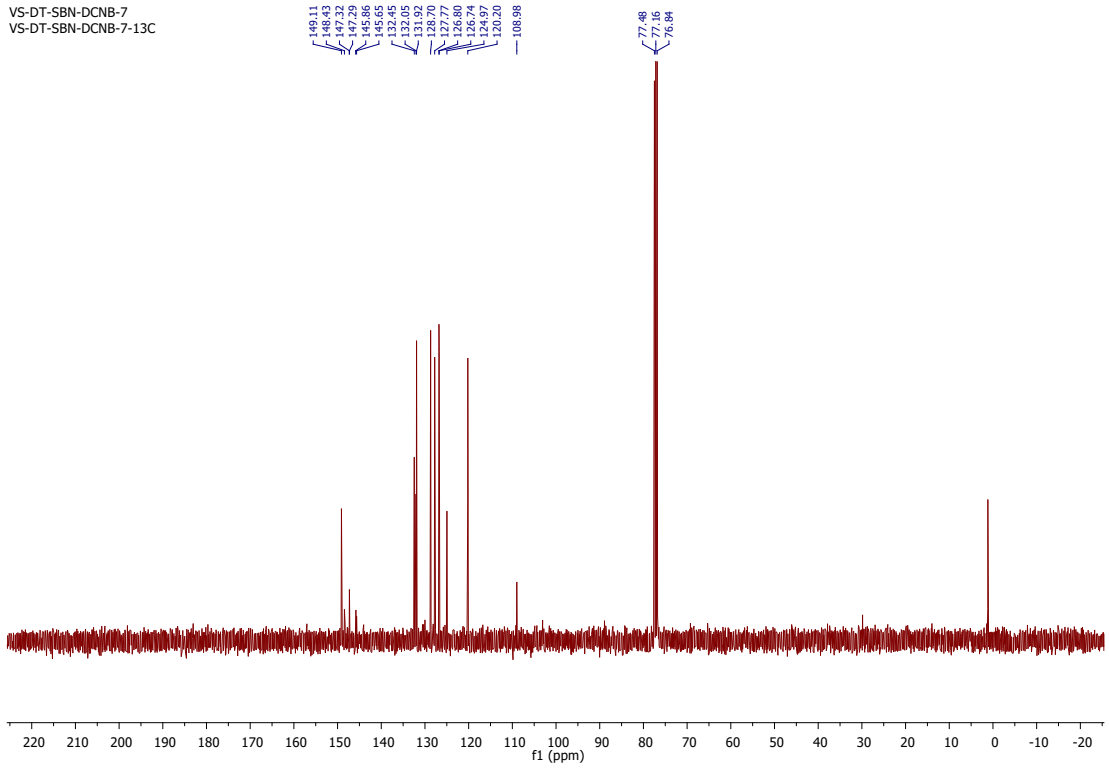

Fig. S5. ^{13}C NMR of SBN-DCNB.

2. RBN-DCNB: ^{1}H NMR (400 MHz, $CDCl_3$) δ 8.08 (d, *J* = 8.9 Hz, 2H), 8.00 (d, *J* = 8.2 Hz, 2H), 7.59 – 7.40 (m, 8H).

^{13}C NMR (100 MHz, $CDCl_3$) δ 149.11, 148.40, 148.27, 145.80, 145.67, 132.45, 132.05, 131.92, 128.70, 127.77, 126.79, 126.74, 124.97, 120.19, 108.98.

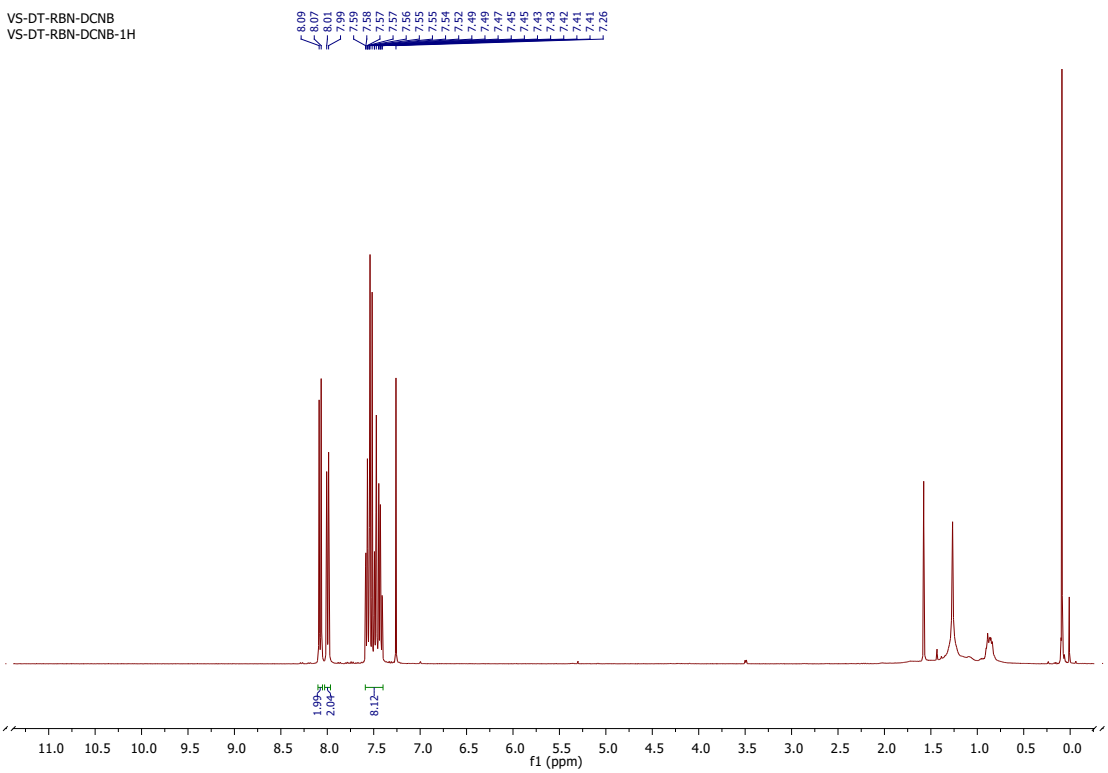

Fig. S6. ^{1}H NMR of RBN-DCNB. (peaks at 0.9 and 1.3 correspond to grease; peak at 1.6 corresponds to moisture in $CDCl_3$)

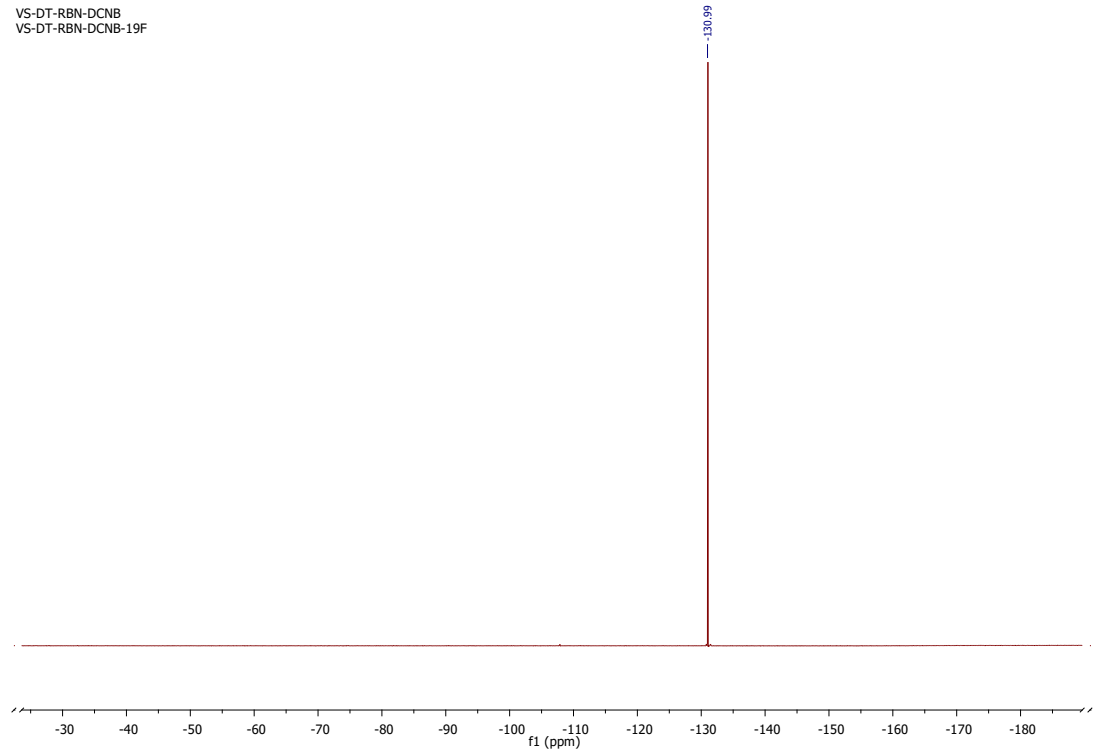

Fig. S7. ^{19}F NMR of RBN-DCNB.

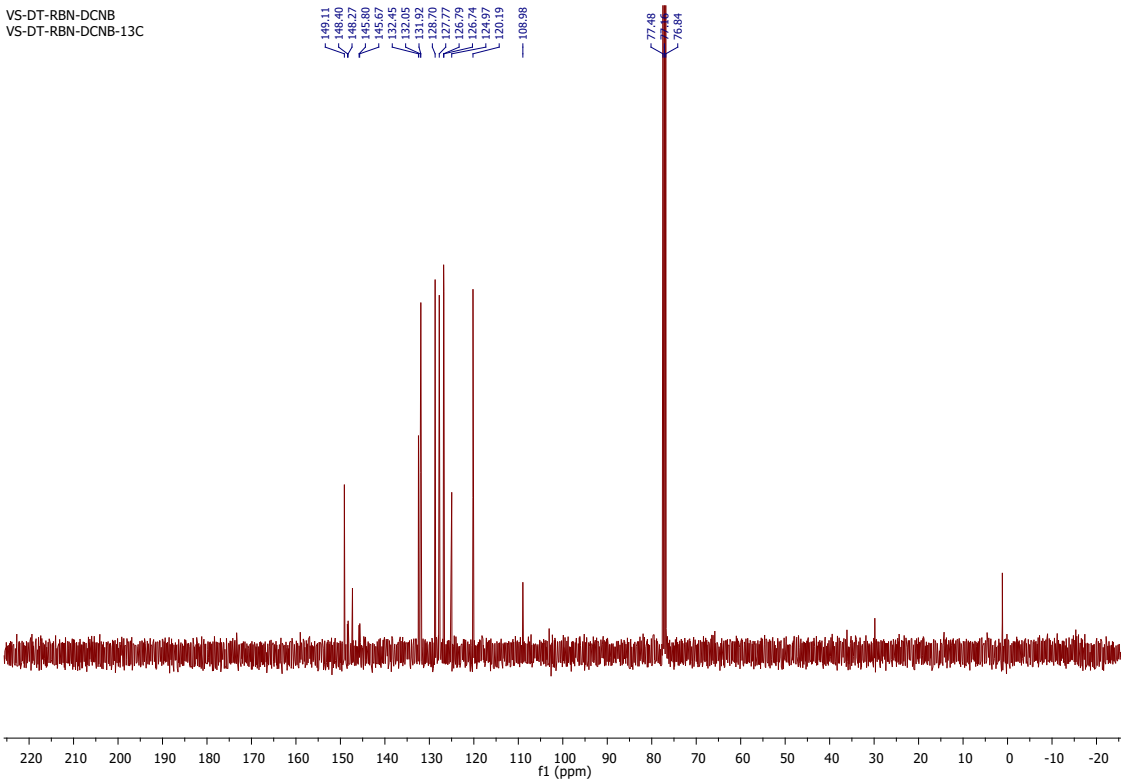

Fig. S8. ^{19}C NMR of RBN-DCNB.

3. CZ4BTXY: ^{1}H NMR (400 MHz, $CDCl_3$) δ 8.32 (d, *J* = 7.8 Hz, 1H), 7.38 – 7.17 (m, 4H), 6.92 (d, *J* = 8.1 Hz, 1H), 6.63 (d, *J* = 8.0 Hz, 1H), 4.19 (t, *J* = 6.4 Hz, 2H), 1.97 – 1.87 (m, 2H), 1.69 – 1.56 (m, 2H), 1.02 (t, *J* = 7.4 Hz, 3H).

^{13}C NMR (100 MHz, $CDCl_3$) δ 155.87, 141.01, 138.79, 126.78, 124.94, 123.14, 122.88, 119.68, 112.75, 110.04, 103.36, 101.14, 67.74, 31.67, 19.63, 14.08.

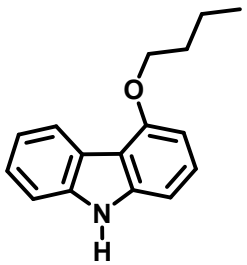

CZ4BTXY

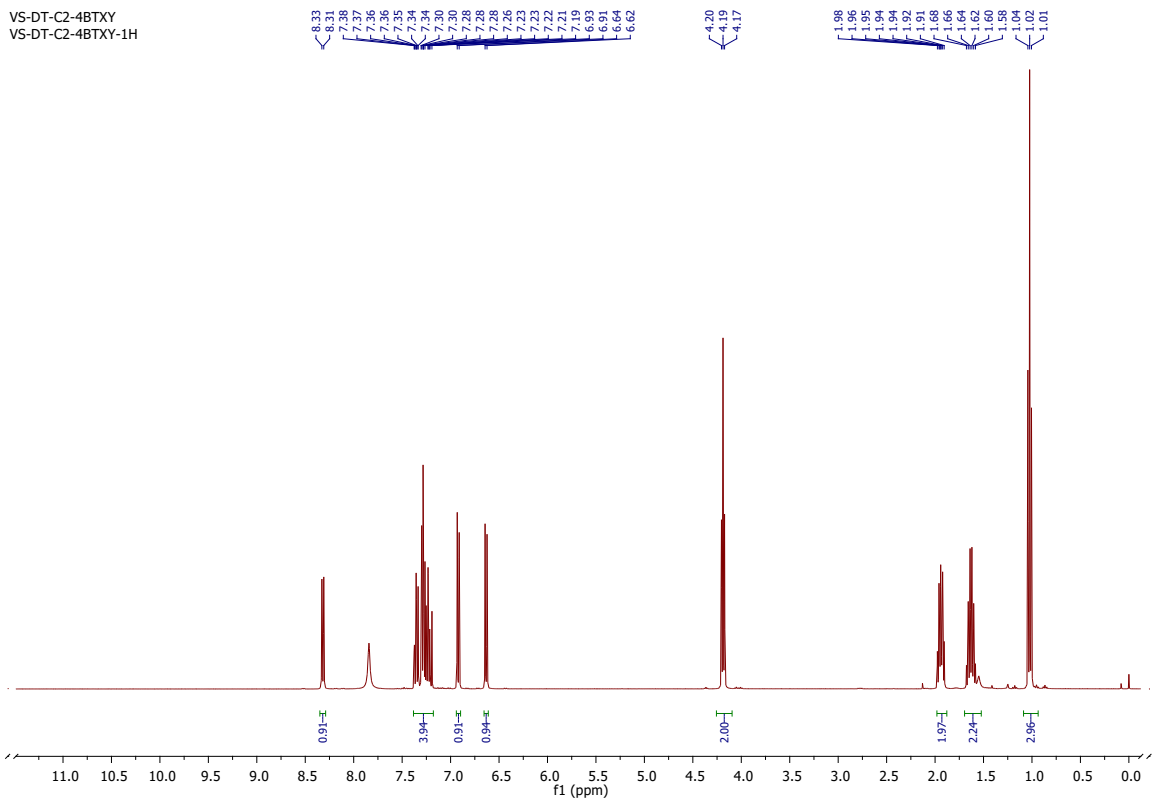

Fig. S9. ^{1}H NMR of CZ4BTXY.

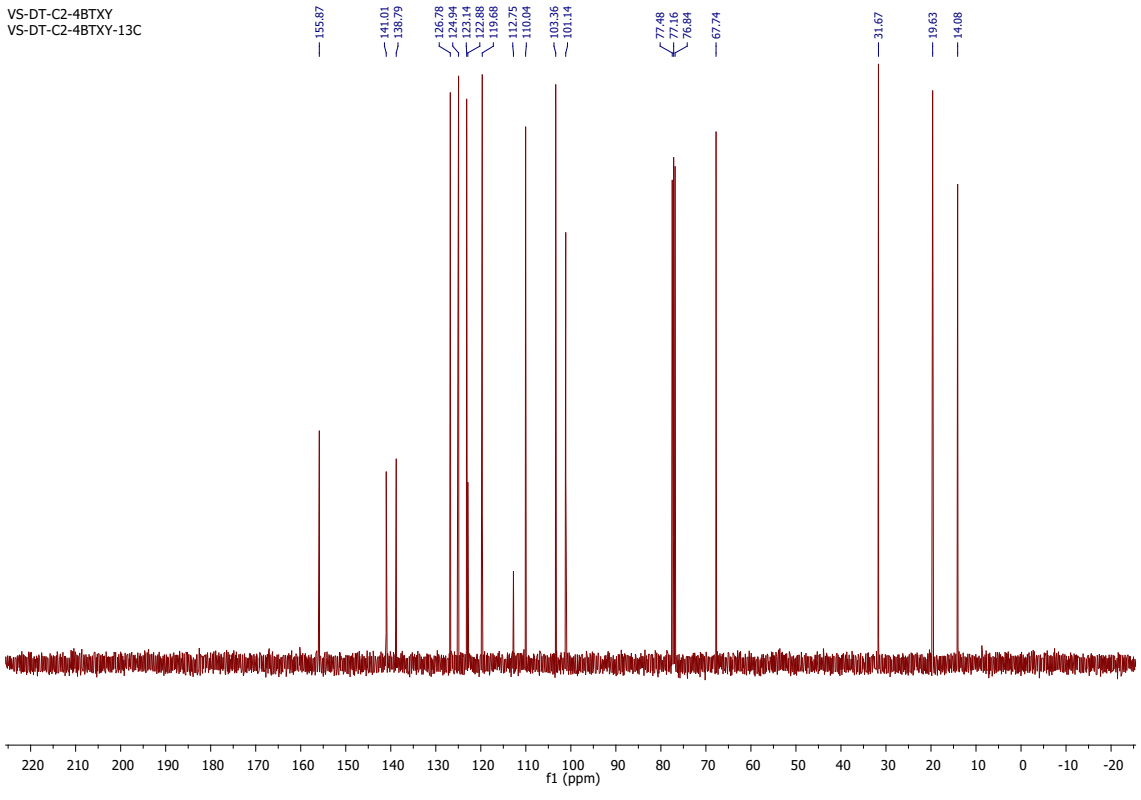

Fig. S10. ^{13}C NMR of CZ4BTXY.

4. *S*-CZ4BTXY

^{1}H NMR (400 MHz, $CDCl_3$) δ 8.14 – 7.91 (m, 6H), 7.71 (d, *J* = 8.8 Hz, 2H), 7.61 – 7.49 (m, 4H), 7.48 – 7.40 (m, 2H), 7.24 – 7.10 (m, 4H), 6.97 (dt, *J* = 7.8, 4.2 Hz, 1H), 6.86 – 6.73 (m, 4H), 6.59 (t, *J* = 8.2 Hz, 1H), 6.49 – 6.36 (m, 2H), 4.12 – 3.94 (m, 4H), 1.83 (tt, *J* = 12.6, 6.4 Hz, 4H), 1.59 – 1.47 (m, 4H), 1.03 – 0.93 (m, 6H).

^{13}C NMR (100 MHz, $CDCl_3$) δ 155.70, 155.65, 155.34, 155.28, 151.35, 149.40, 140.78, 140.29, 138.62, 135.74, 132.54, 132.16, 131.90, 128.72, 127.74, 126.86, 126.71, 126.41, 126.33, 125.06, 124.46, 123.84, 123.79, 123.68, 123.41, 123.34, 122.96, 121.58, 121.35, 120.77, 114.65, 114.61, 113.65, 113.43, 111.69, 109.11, 103.50, 103.43, 103.29, 102.46, 67.77, 31.52, 31.49, 19.51, 14.03.

HRMS (DUAL ESI+VE.m): m/z calculated for $C_{60}H_{44}N_4O_4$ [M+H]+: 885.34; found: 885.3402

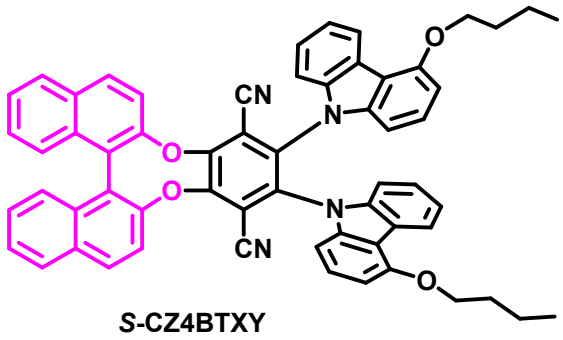

***S*-CZ4BTXY**

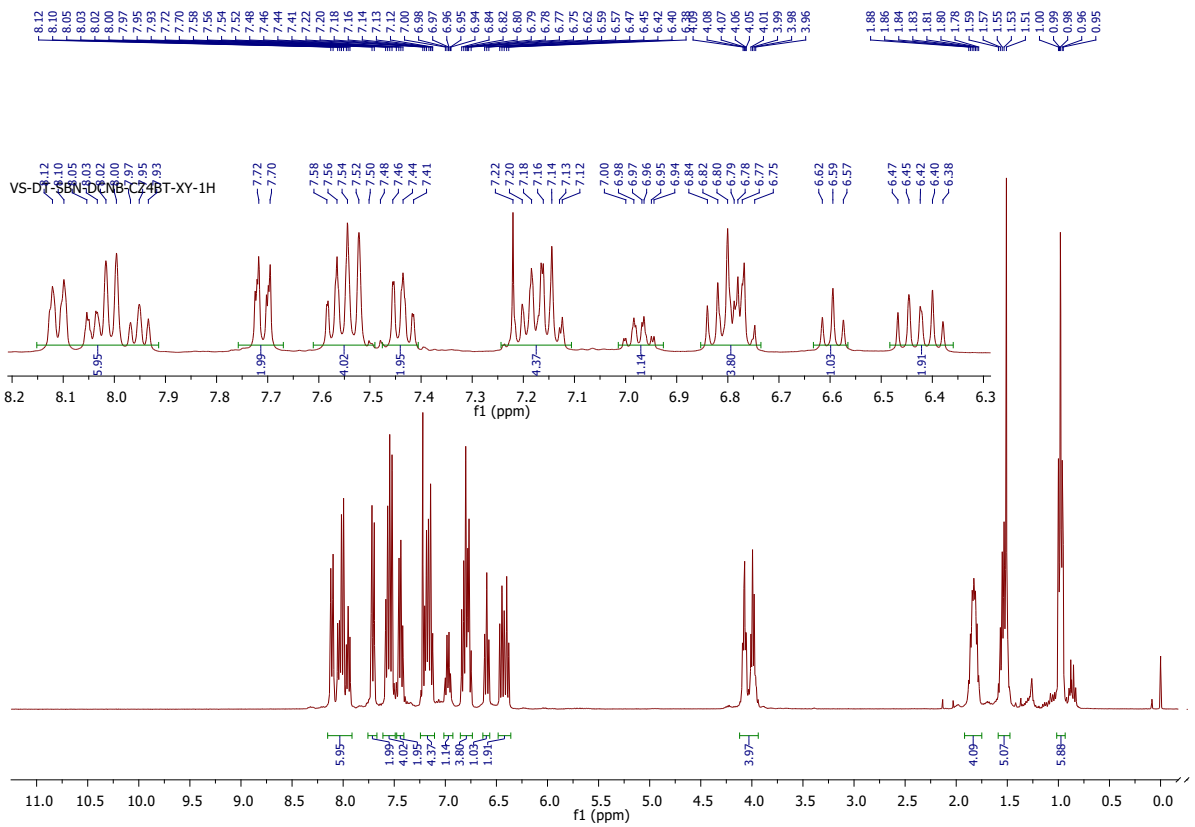

Fig. S11. ^{1}H NMR of S-CZ4BTXY.

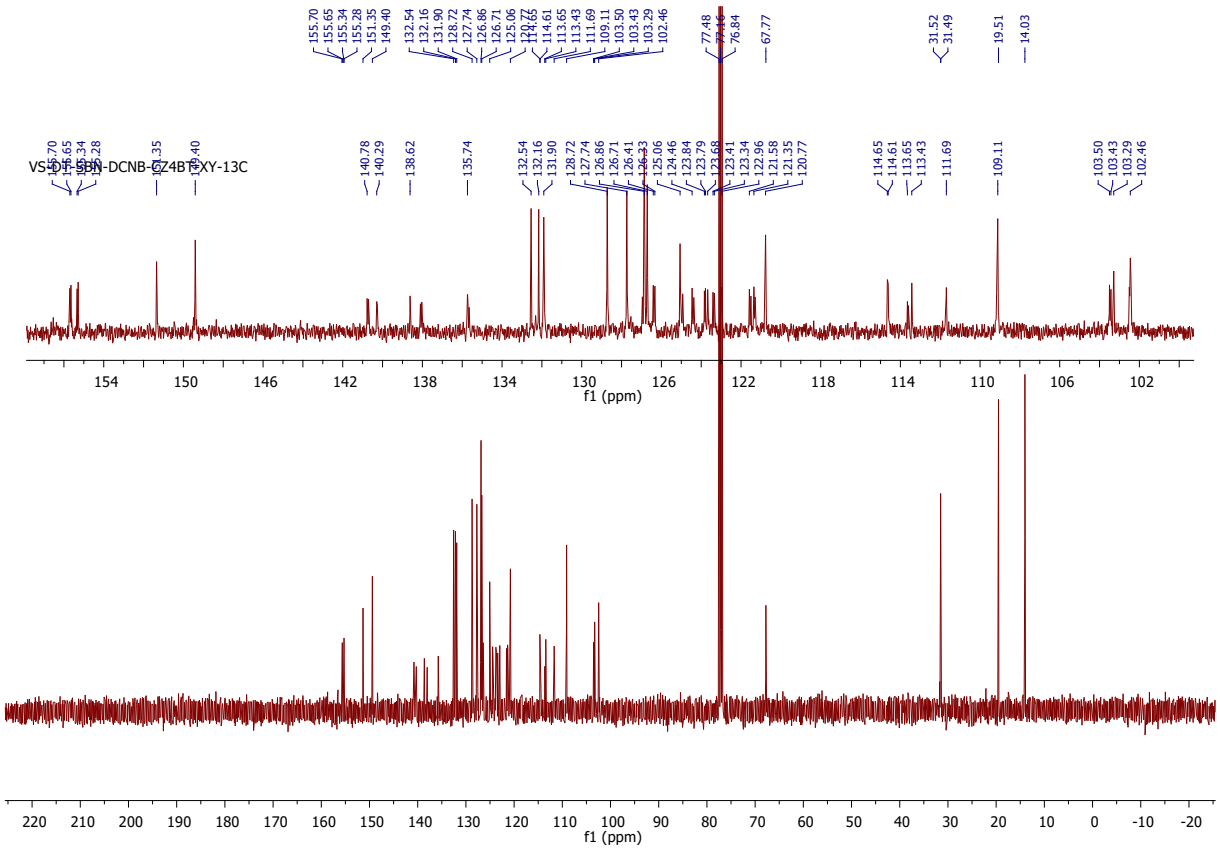

Fig. S12. ^{13}C NMR of S-CZ4BTXY.

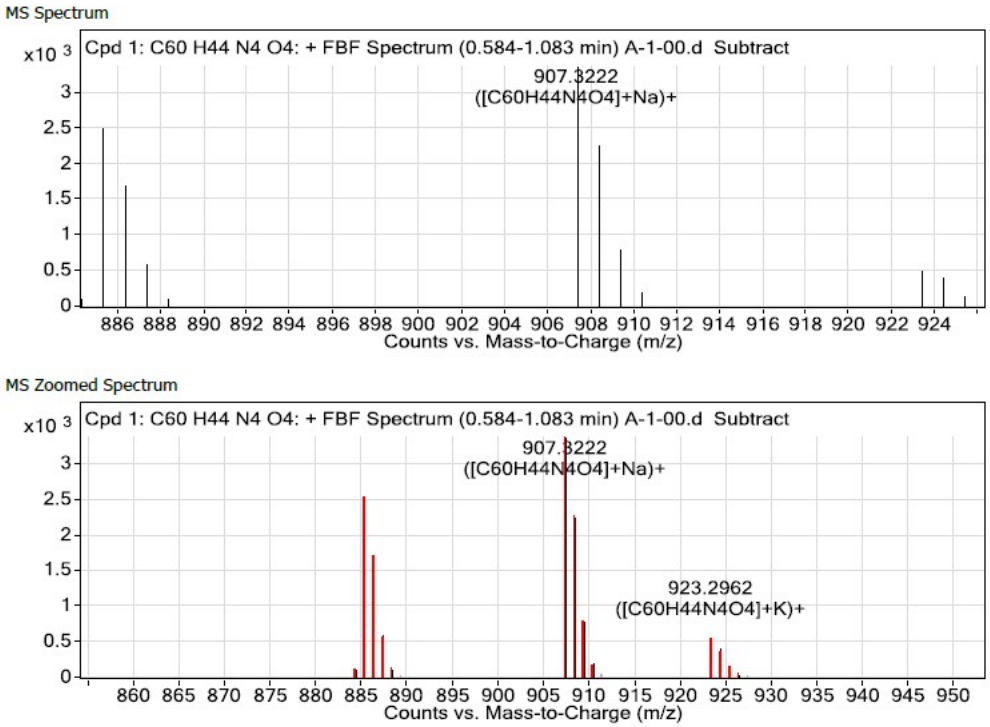

MS Spectrum Peak List

m/z	z	Abund	Formula	Ion
884.3291	1	120.03	C60H44N4O4	M+
885.3402	1	2501.45	C60H44N4O4	(M+H)+
886.343	1	1704.14	C60H44N4O4	(M+H)+
887.3451	1	601.67	C60H44N4O4	(M+H)+
907.3222	1	3362.03	C60H44N4O4	(M+Na)+
908.3243	1	2246.19	C60H44N4O4	(M+Na)+

Fig. S13. HRMS spectra of S-CZ4BTXY.

5. R-CZ4BTXY

^{1}H NMR (400 MHz, $CDCl_3$) δ 7.97 (dd, *J* = 15.7, 8.2 Hz, 3H), 7.87 (dd, *J* = 14.8, 7.6 Hz, 3H), 7.61 (d, *J* = 8.8 Hz, 2H), 7.44 (dd, *J* = 12.4, 5.9 Hz, 4H), 7.38 – 7.28 (m, 2H), 7.15 – 7.00 (m, 4H), 6.87 (dd, *J* = 14.2, 6.6 Hz, 1H), 6.77 – 6.62 (m, 4H), 6.48 (t, *J* = 8.1 Hz, 1H), 6.36 (t, *J* = 8.5 Hz, 1H), 6.28 (t, *J* = 8.0 Hz, 1H), 4.02 – 3.79 (m, 4H), 1.72 (dd, *J* = 12.9, 6.4 Hz, 4H), 1.48 – 1.36 (m, 4H), 0.88 (t, *J* = 5.8 Hz, 6H).

^{13}C NMR (100 MHz, $CDCl_3$) δ 155.69, 155.64, 155.32, 155.27, 151.35, 149.40, 140.77, 140.70, 140.29, 140.26, 138.62, 138.59, 138.10, 138.03, 135.74, 135.66, 132.53, 132.14, 131.90, 128.71, 127.72, 126.96, 126.84, 126.69, 126.41, 126.33, 125.05, 124.93, 124.45, 124.36, 123.83, 123.78, 123.65, 123.40, 123.34, 123.00, 122.96, 121.57, 121.49, 121.34, 121.29, 120.75, 114.65, 114.61, 113.63, 113.58, 113.41, 111.69, 109.16, 109.11, 103.50, 103.43, 103.29, 102.45, 67.75, 67.71, 31.50, 31.47, 19.49, 14.02.

HRMS (DUAL ESI+VE.m): m/z calculated for $C_{60}H_{44}N_4O_4$ [M+H]+: 885.34; found: 885.3398

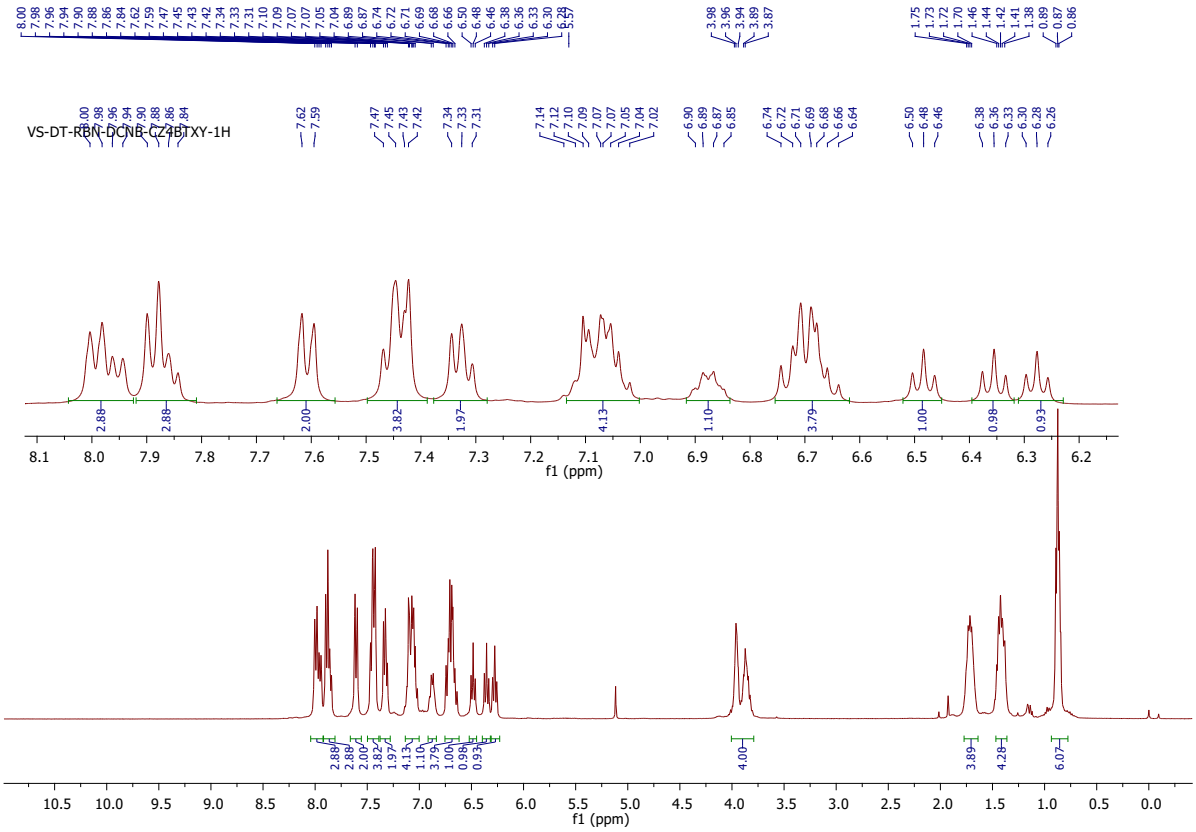

Fig. S14. ^{1}H NMR of R-CZ4BTXY.

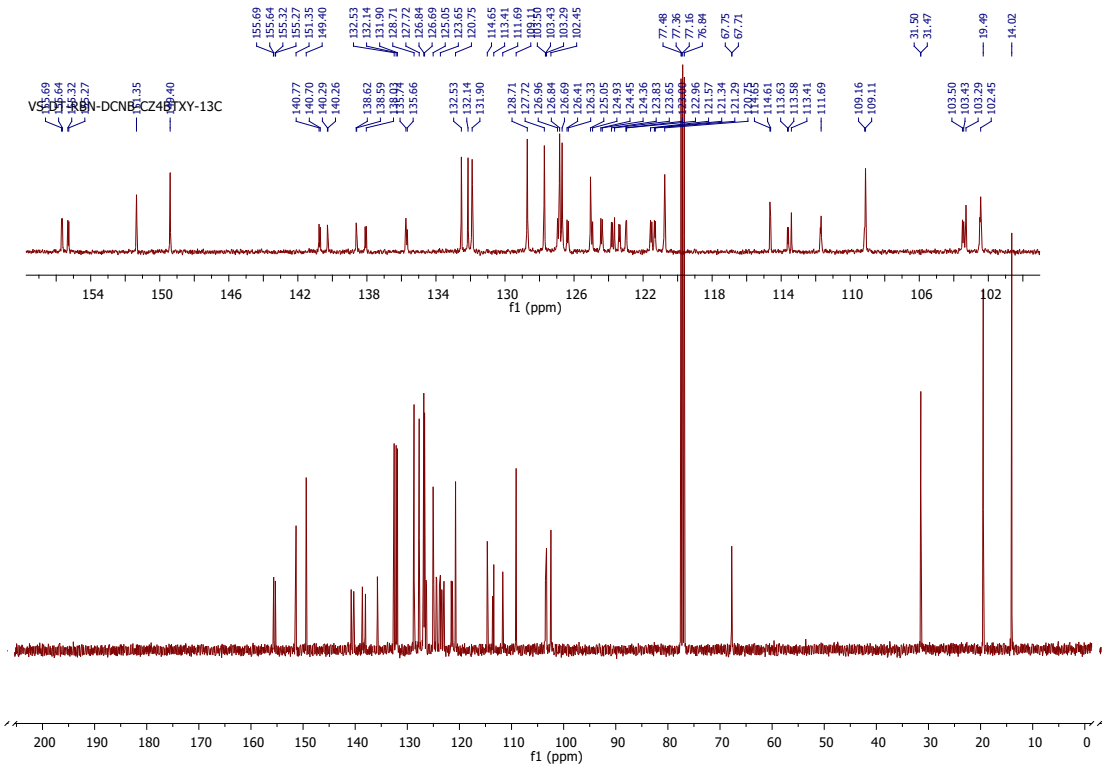

Fig. S15. ^{13}C NMR of RBN-CZ4BTXY.

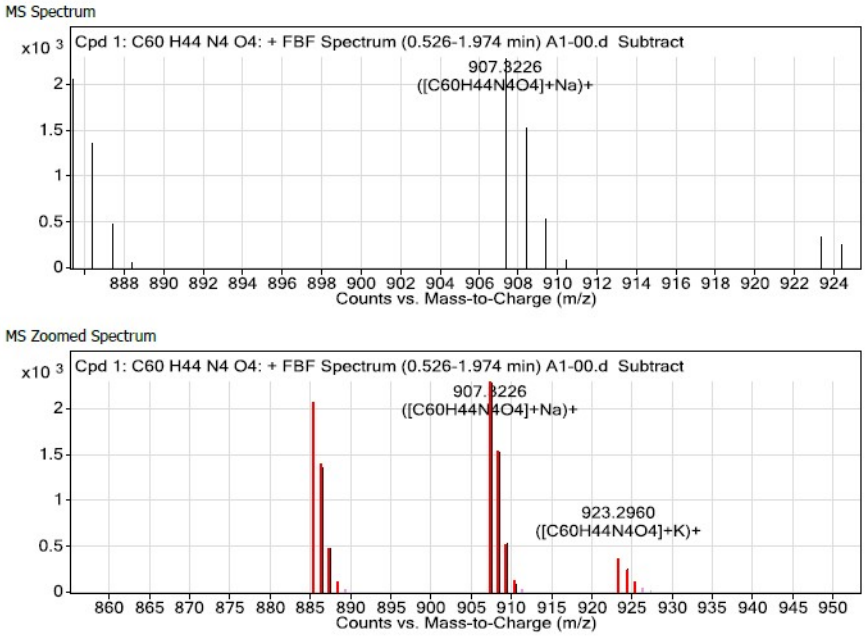

MS Spectrum Peak List

m/z	z	Abund	Formula	Ion
885.3398	1	2068.94	C60H44N4O4	(M+H)+
886.344	1	1366.14	C60H44N4O4	(M+H)+
887.3476	1	482.63	C60H44N4O4	(M+H)+
907.3226	1	2288.17	C60H44N4O4	(M+Na)+
908.3258	1	1530.3	C60H44N4O4	(M+Na)+
909.327	1	543.44	C60H44N4O4	(M+Na)+

Fig. S16. HRMS spectra of R-CZ4BTXY.

6. ***S*-CZ4OH:**

^{1}H NMR (400 MHz, $CDCl_3$) δ 8.11 (d, *J* = 8.8 Hz, 2H), 8.00 (d, *J* = 8.2 Hz, 2H), 7.70 (d, *J* = 8.8 Hz, 2H), 7.54 (dd, *J* = 15.8, 7.8 Hz, 4H), 7.46 – 7.38 (m, 2H), 7.22 – 6.94 (m, 7H), 6.70 (s, 5H), 6.31 (s, 2H).

^{13}C NMR (100 MHz, $CDCl_3$) δ 149.63, 146.57, 141.24, 138.46, 132.42, 132.18, 131.82, 128.68, 127.60, 126.86, 126.54, 125.58, 125.21, 124.99, 122.56, 120.67, 119.11, 112.98, 111.27, 106.91.

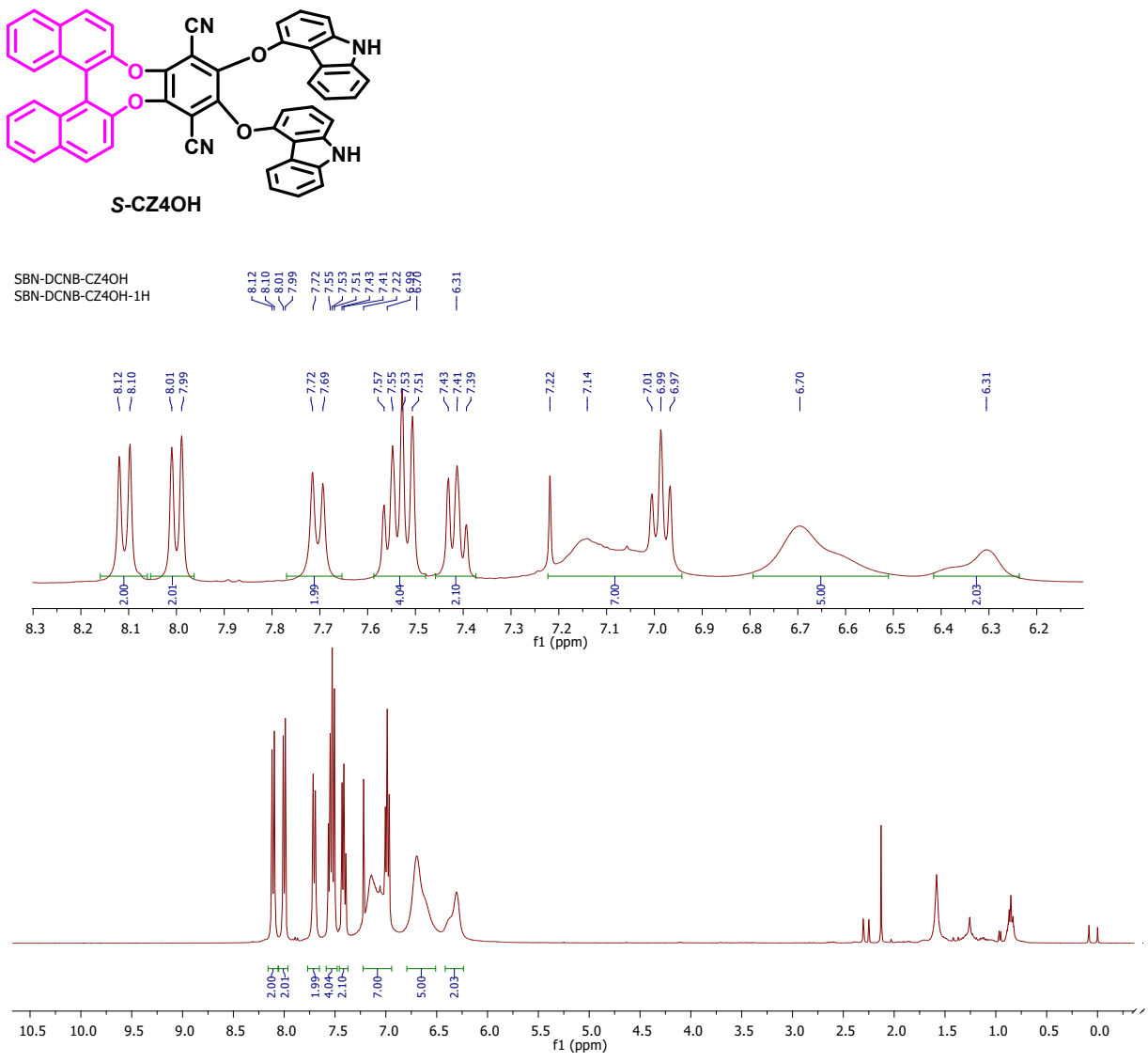

Fig. S17. ^{1}H NMR of S-CZ4OH. (peaks at 0.9 and 1.3 correspond to grease; peak at 1.6 corresponds to moisture in $CDCl_3$; peak at 2.2 corresponds to acetone)

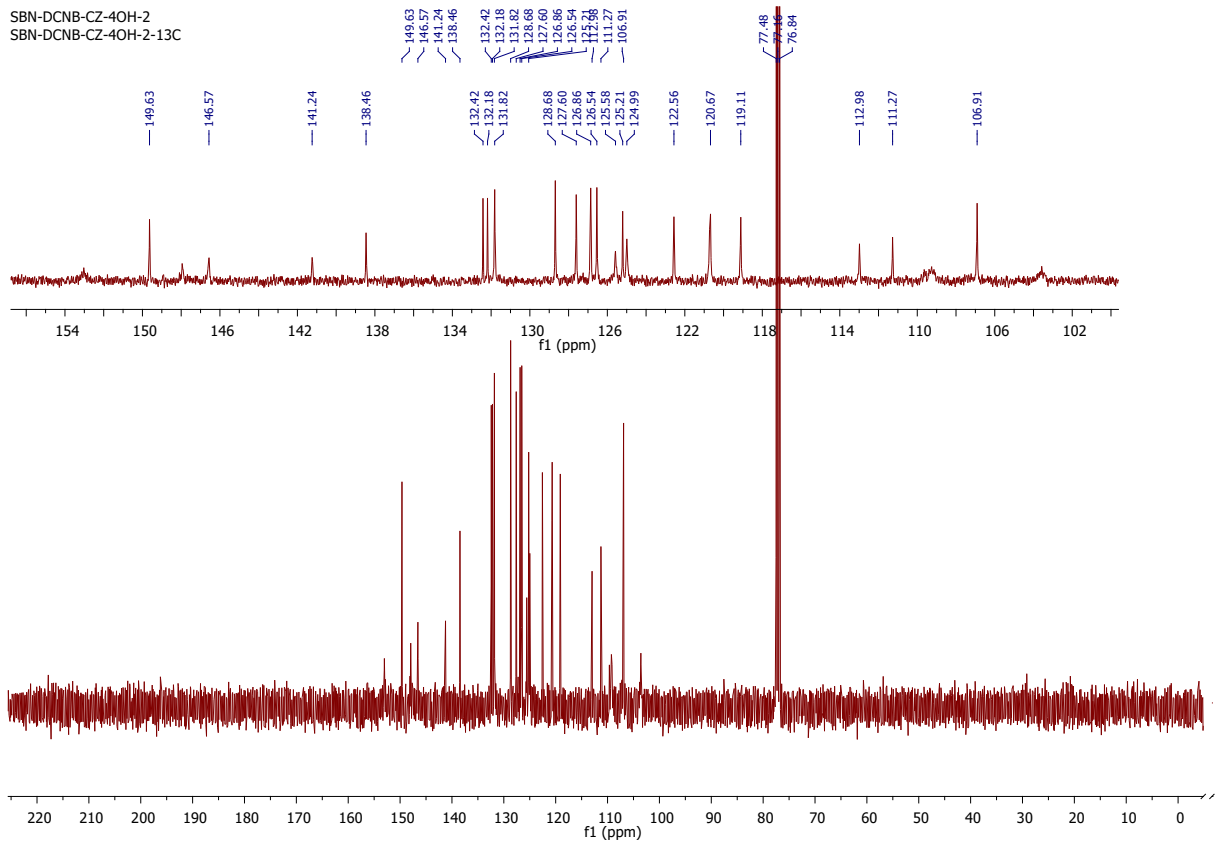

Fig. S18. ^{13}C NMR of *S*-CZ4OH.

7. R-CZ4OH:

^{1}H NMR (400 MHz, $CDCl_3$) δ 8.15 (d, *J* = 8.9 Hz, 2H), 8.04 (d, *J* = 8.2 Hz, 2H), 7.75 (d, *J* = 8.8 Hz, 2H), 7.58 (dd, *J* = 14.3, 7.4 Hz, 4H), 7.48 – 7.41 (m, 2H), 7.28 (d, *J* = 18.2 Hz, 2H), 7.02 (t, *J* = 7.6 Hz, 4H), 6.86 – 6.27 (m, 8H).

^{13}C NMR (100 MHz, $CDCl_3$) δ 162.69, 149.59, 146.54, 141.24, 138.46, 132.38, 132.14, 131.80, 128.67, 127.59, 126.82, 126.52, 125.53, 125.17, 124.96, 122.51, 120.62, 119.04, 112.91, 111.27, 106.91.

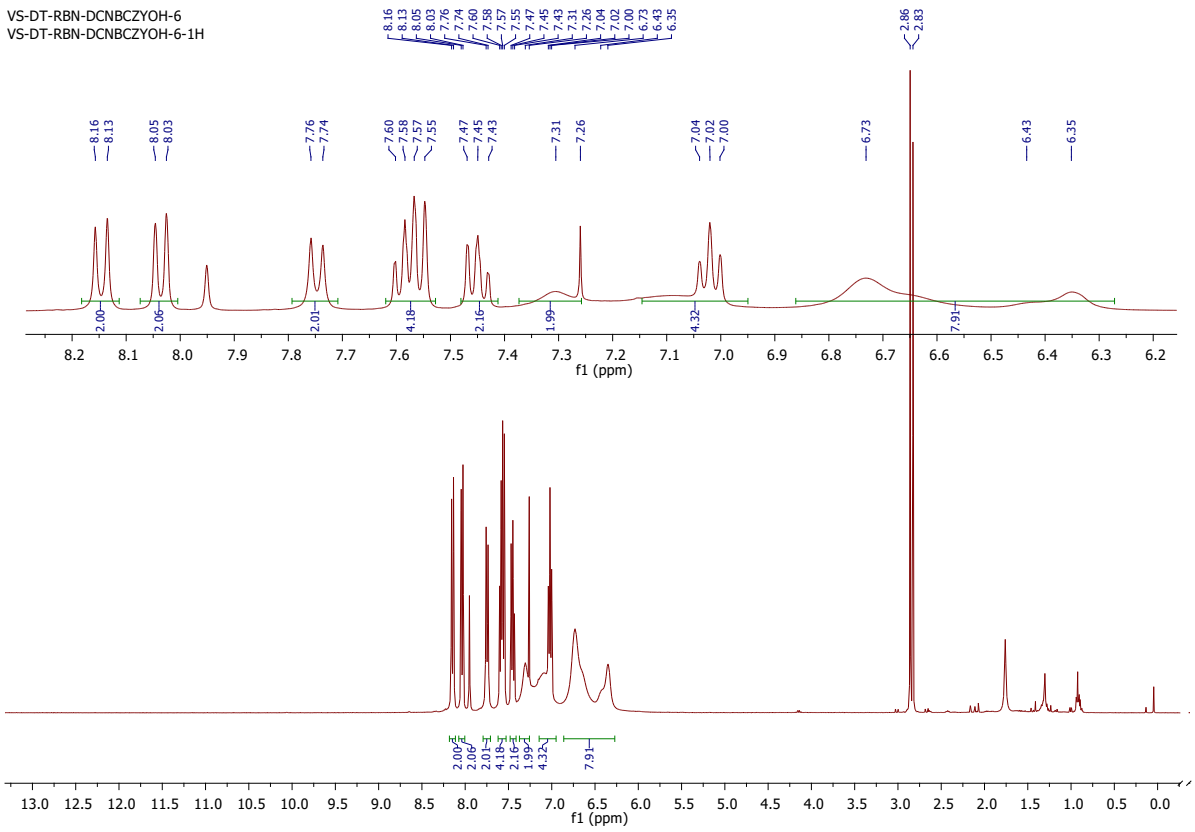

Fig.S19. ^{1}H NMR of R-CZ4OH. (The peak at 2.86, 2.83 and 7.95 shows DMF solvent is present. We have directly used this material for the next step.)

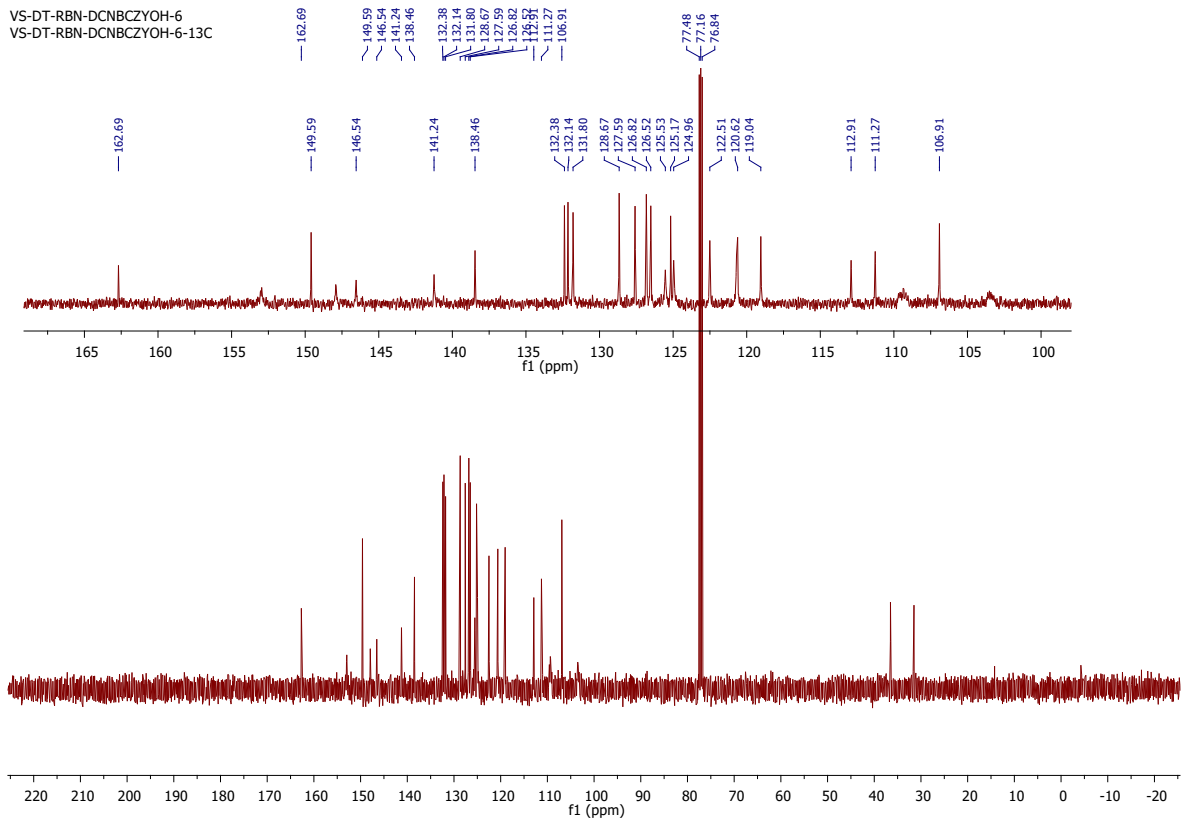

Fig. S20. ^{13}C NMR of R-CZ4OH. (The peaks between 30 and 40 shows DMF solvent is present. We have directly used this material for the next step.)

8. S-NBTOCZ

^{1}H NMR (400 MHz, $CDCl_3$) δ 8.16 (d, *J* = 8.8 Hz, 2H), 8.05 (d, *J* = 8.2 Hz, 2H), 7.75 (d, *J* = 8.8 Hz, 2H), 7.62 – 7.51 (m, 4H), 7.49 – 7.42 (m, 2H), 7.25 – 6.99 (m, 6H), 6.93 (d, *J* = 6.0 Hz, 2H), 6.75 (dd, *J* = 36.1, 7.0 Hz, 4H), 6.34 (t, *J* = 16.0 Hz, 2H), 3.78 (s, 4H), 1.54 (p, *J* = 7.2 Hz, 4H), 1.33 – 1.21 (m, 4H), 0.91 (t, *J* = 7.3 Hz, 6H).

^{13}C NMR (100 MHz, $CDCl_3$) δ 153.42, 149.71, 147.94, 146.59, 142.16, 139.28, 132.46, 132.24, 131.81, 128.70, 127.60, 126.92, 126.53, 125.43, 125.26, 124.59, 122.83, 120.83, 120.42, 118.53, 112.44, 111.25, 109.87, 107.06, 104.82, 42.79, 31.08, 20.55, 14.01.

HRMS (DUAL ESI+VE.m): m/z calculated for $C_{60}H_{44}N_4O_4$ [M+H]+: 885.34; found: 885.3392

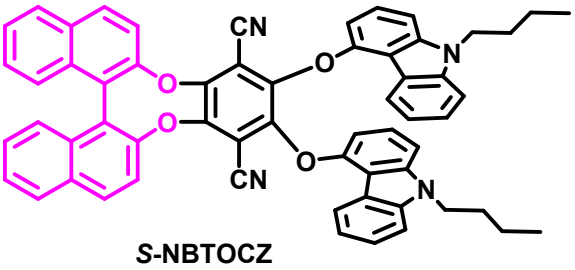

S-NBTOCZ

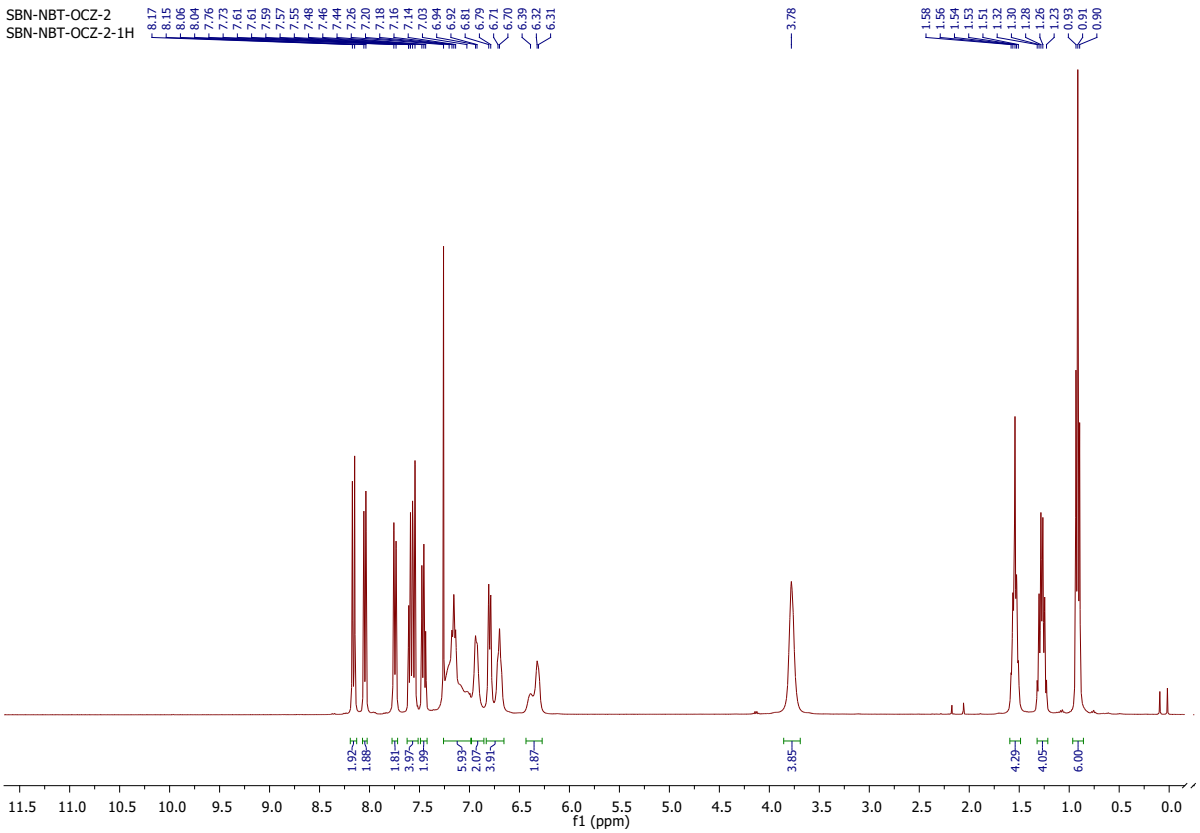

Fig. S21. ^{1}H NMR of S-NBTOCZ.

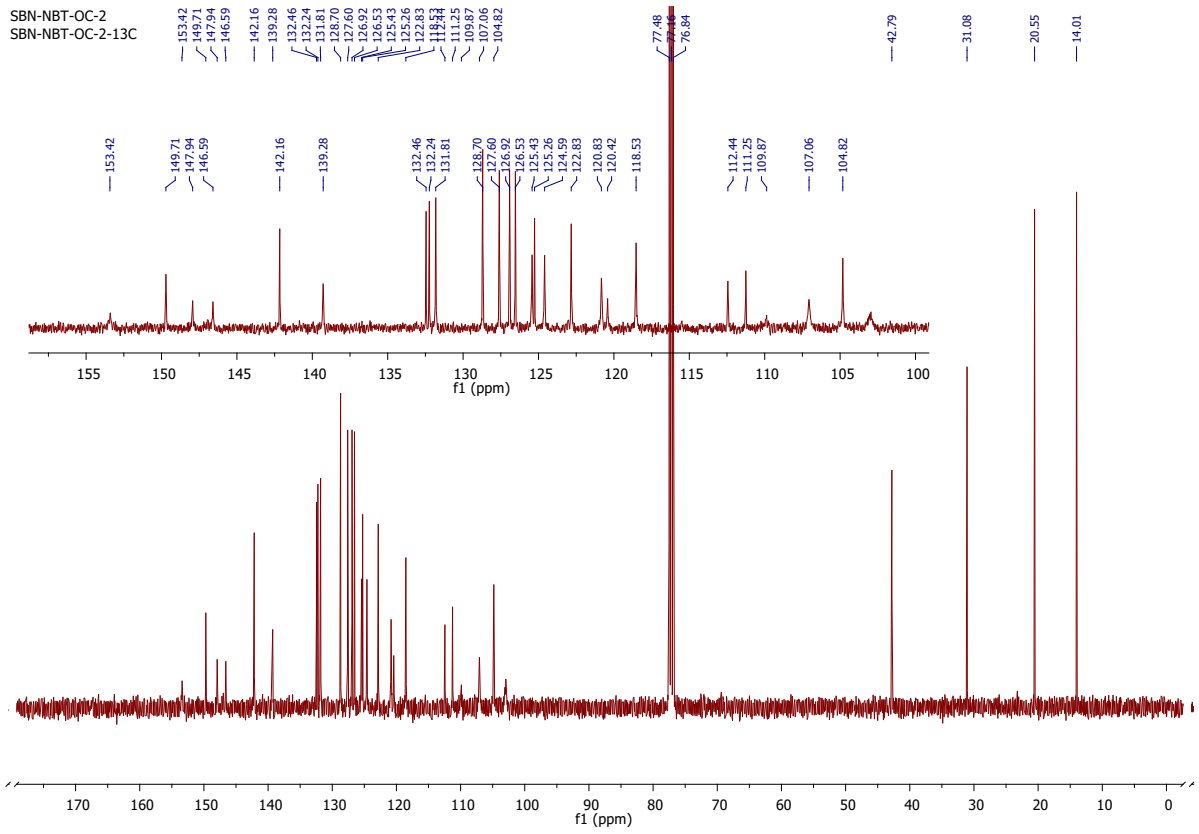

Fig. S22. ^{13}C NMR of S-NBTOCZ.

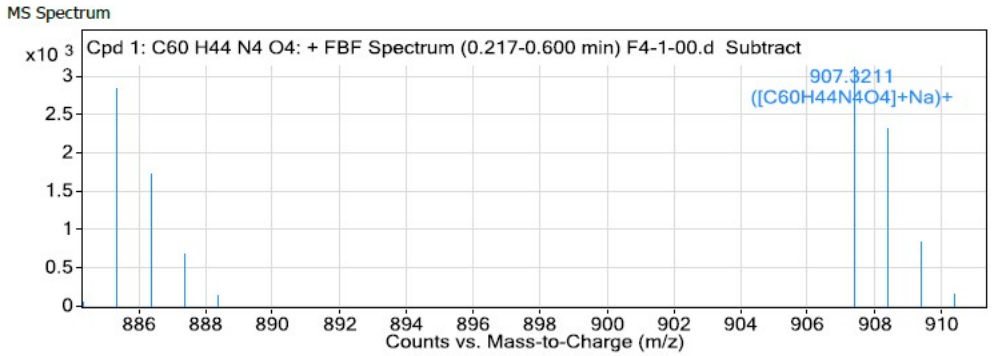

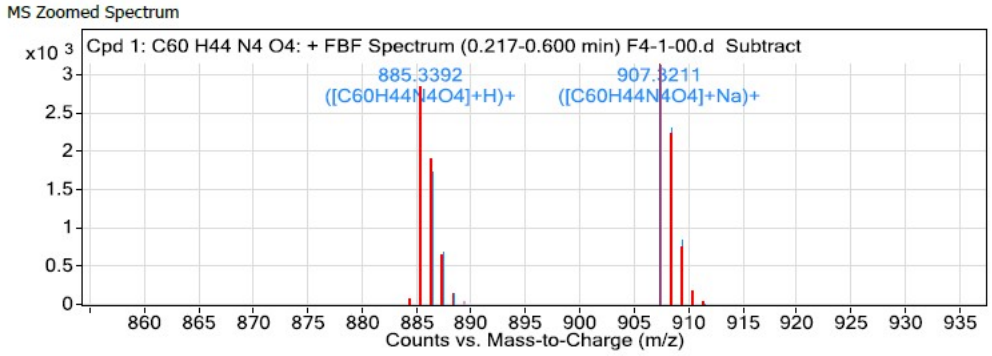

MS Spectrum Peak List

m/z	z	Abund	Formula	Ion
884.3317	1	67.39	C60H44N4O4	M+
885.3392	1	2841.07	C60H44N4O4	(M+H)+
886.343	1	1736.7	C60H44N4O4	(M+H)+
887.3462	1	695	C60H44N4O4	(M+H)+
888.3454	1	155.35	C60H44N4O4	(M+H)+
907.3211	1	3134.07	C60H44N4O4	(M+Na)+

Fig. S23. HRMS spectra of S-NBTOCZ.

9. R-NBTOCZ

^{1}H NMR (400 MHz, $CDCl_3$) δ 8.16 (d, *J* = 8.8 Hz, 2H), 8.05 (d, *J* = 8.2 Hz, 2H), 7.74 (d, *J* = 8.8 Hz, 2H), 7.58 (dd, *J* = 17.1, 8.7 Hz, 4H), 7.49 – 7.41 (m, 2H), 7.12 (dd, *J* = 33.5, 26.3 Hz, 6H), 6.93 (d, *J* = 5.6 Hz, 2H), 6.80 (d, *J* = 8.0 Hz, 2H), 6.71 (d, *J* = 6.1 Hz, 2H), 6.34 (t, *J* = 16.3 Hz, 2H), 3.78 (s, 4H), 1.61 – 1.48 (m, 4H), 1.27 (dq, *J* = 14.8, 7.3 Hz, 4H), 0.91 (t, *J* = 7.3 Hz, 6H).

^{13}C NMR (100 MHz, $CDCl_3$) δ 153.37, 149.70, 147.93, 146.57, 142.16, 139.27, 132.45, 132.23, 131.81, 128.70, 127.59, 126.91, 126.53, 125.43, 125.26, 124.59, 122.83, 120.81, 120.41, 118.53, 112.44, 111.25, 107.05, 104.82, 42.79, 31.07, 20.55, 14.01.

HRMS (DUAL ESI+VE.m): m/z calculated for $C_{60}H_{44}N_4O_4$ [M+H]+: 885.34; found: 885.34

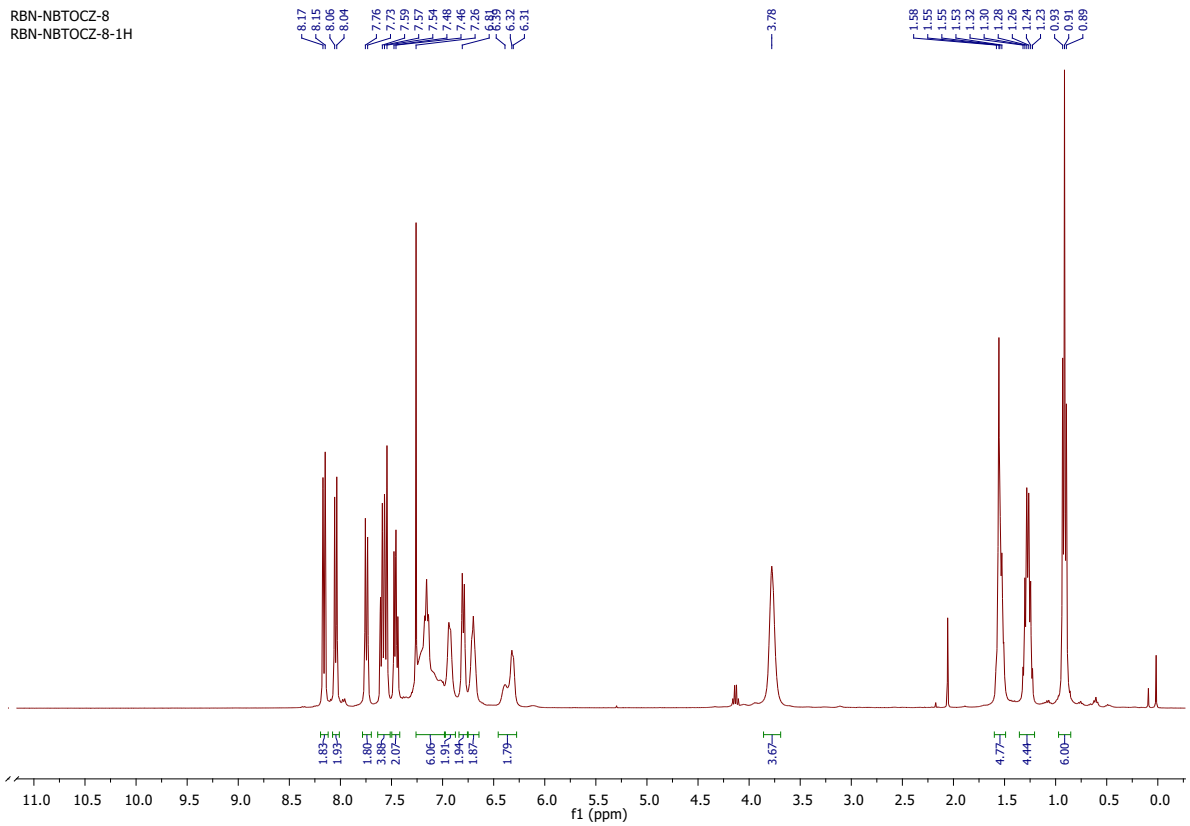

Fig. S24. ^{1}H NMR of R-NBTOCZ.

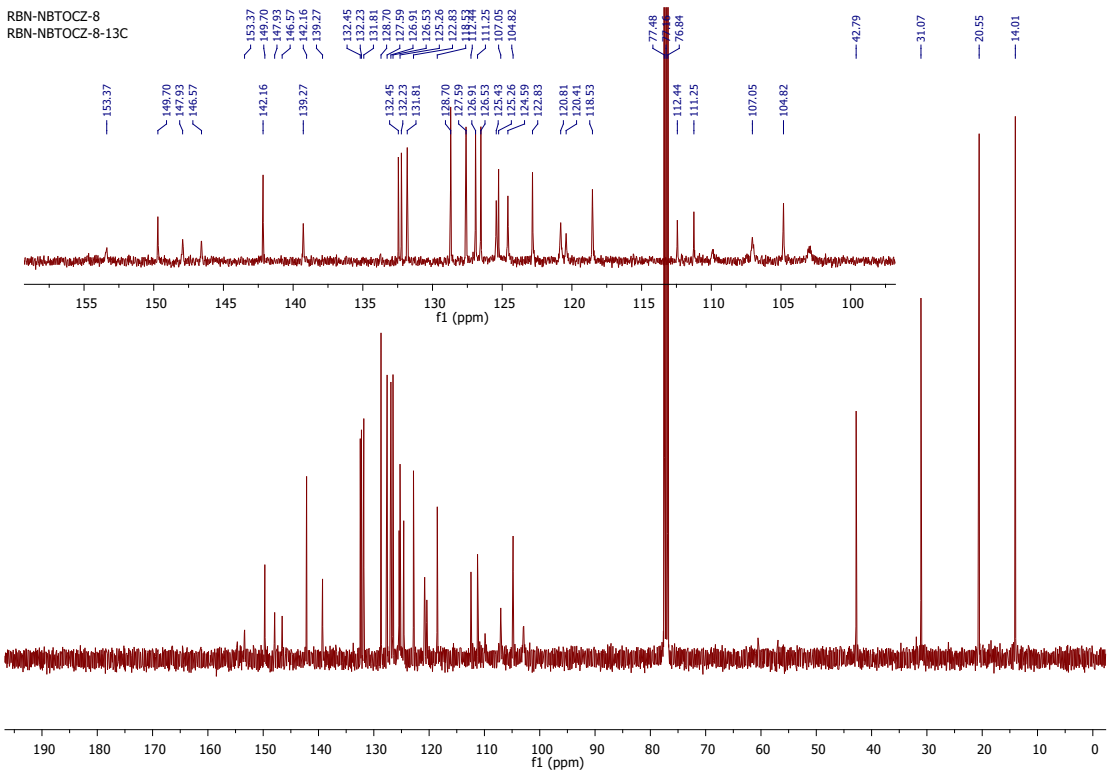

Fig. S25. ^{13}C NMR of R-NBTOCZ.

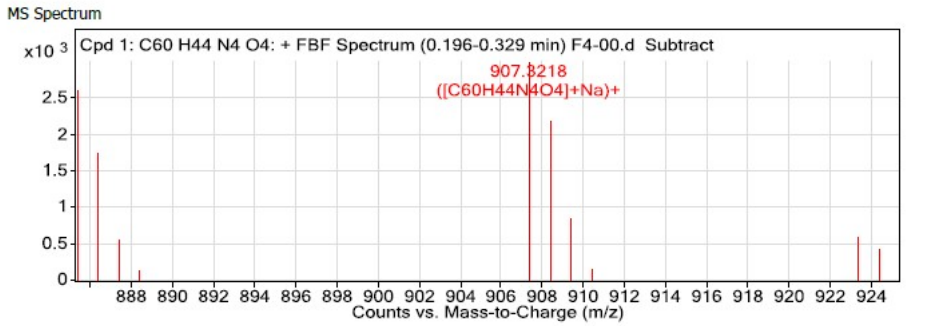

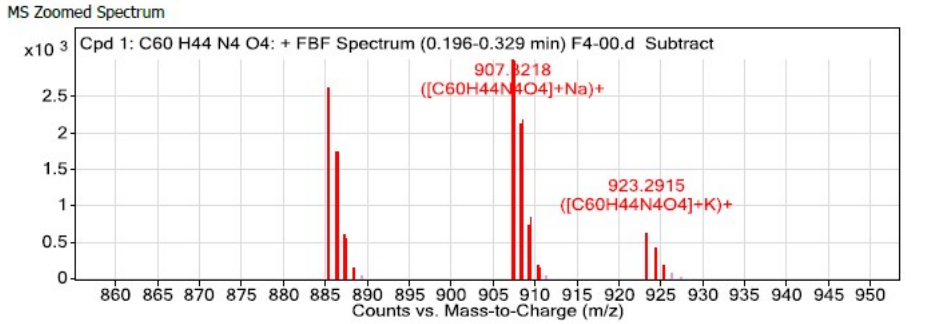

MS Spectrum Peak List

m/z	z	Abund	Formula	Ion
885.34	1	2613.55	C60H44N4O4	(M+H)+
886.3429	1	1753.37	C60H44N4O4	(M+H)+
887.3486	1	574.08	C60H44N4O4	(M+H)+
907.3218	1	2999	C60H44N4O4	(M+Na)+
908.3257	1	2194.6	C60H44N4O4	(M+Na)+
909.3283	1	862.87	C60H44N4O4	(M+Na)+

Fig. S26. HRMS spectra of R-NBTOCZ.

High-Performance Liquid Chromatography (HPLC)

High-Performance Liquid Chromatography (HPLC) analyses were performed on a Shimadzu UFLC (Ultra-Fast Liquid Chromatograph) system, equipped with an LC-20AD pump, SPD-M20A Diode Array Detector (DAD), and CBM-20A communications bus module. All samples were prepared by dissolving approximately 2 mg of the compound in 5 mL of HPLC-grade acetonitrile (ACN). Chiral separations were achieved using a DAICEL CHIRALPAK AD-H (column 4.6 mm × 10 mm). The column was maintained at 25 °C. The injection volume was 15 µL. All separations used a total flow rate of 1.0 mL/min. For the O-linkage isomers (R/S-NBTOCZ), analysis was performed using an isocratic mobile phase of 95:05 (v/v) n-Hexane: Isopropanol (IPA). For the N-linkage samples (R/S-CZ4BTXY), analysis was performed using an isocratic mobile phase of 90:10 (v/v) n-Hexane: Isopropanol (IPA). Detection was carried out using the DAD, and chromatograms were monitored at 300 nm.

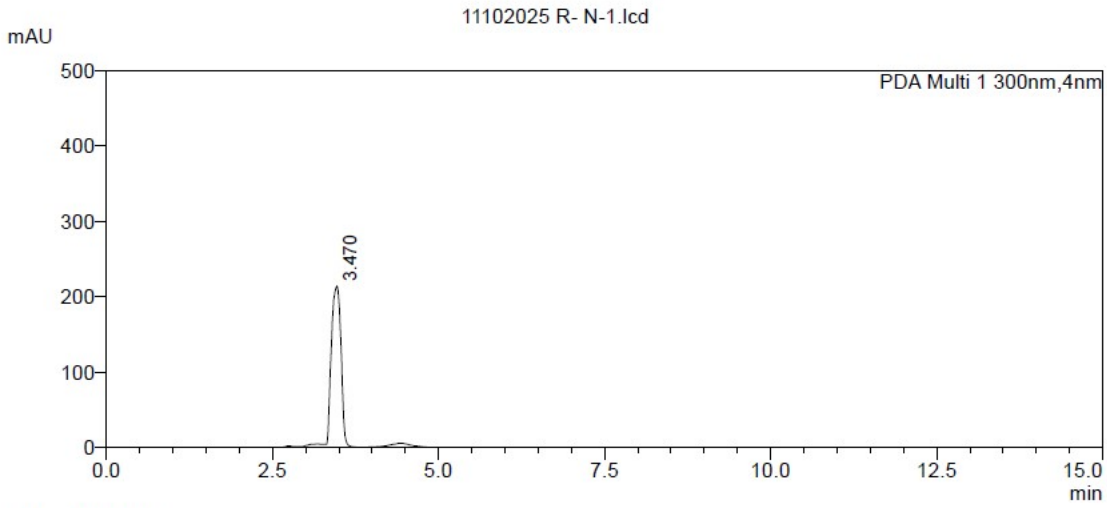

<Peak Table>

PDA Ch1 300nm

Peak#	Ret. Time	Area	Height	Conc.	Unit	Mark	Name
1	3.470	2082955	210316	100.000		M	
Total		2082955	210316				

Fig. S27. HPLC of R-CZ4BTXY.

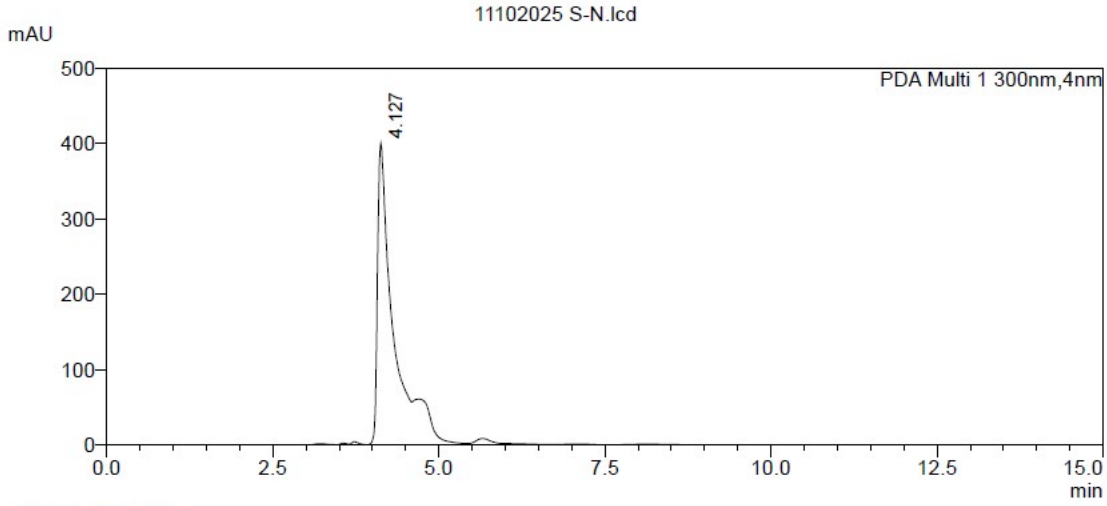

<Peak Table>

PDA Ch1 300nm

Peak#	Ret. Time	Area	Height	Conc.	Unit	Mark	Name
1	4.127	4739296	386224	100.000		M	
Total		4739296	386224				

Fig. S28. HPLC of S-CZ4BTXY.

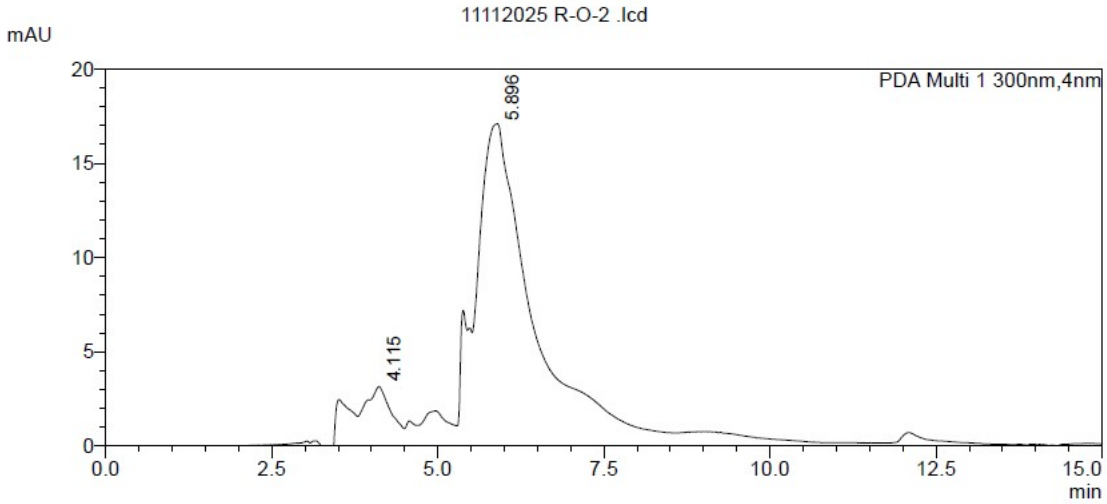

<Peak Table>

PDA Ch1 300nm

Peak#	Ret. Time	Area	Height	Conc.	Unit	Mark	Name
1	4.115	31362	1760	4.482		M	
2	5.896	668404	15260	95.518		M	
Total		699766	17020				

Fig. S29. HPLC of R-NBTOCZ.

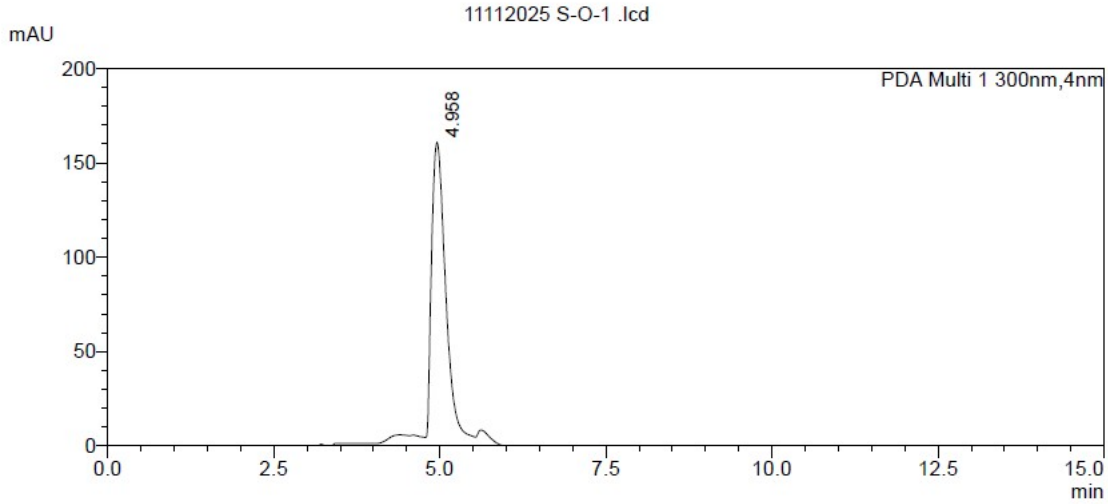

<Peak Table>

PDA Ch1 300nm

Peak#	Ret. Time	Area	Height	Conc.	Unit	Mark	Name
1	4.958	2237890	156429	0.000		M	
Total		2237890	156429				

Fig. S30. HPLC of S-NBTOCZ.

Coordinates for optimized geometry of R-CZ4BTXY.

112

symmetry c1

C	-6.699157000	0.168739000	1.392874000
C	-6.719436000	-0.362247000	2.726299000
C	-5.671964000	-1.220981000	3.152809000
C	-4.631293000	-1.533087000	2.312360000
C	-4.622298000	-1.002194000	1.005992000
C	-5.627869000	-0.196295000	0.509421000
C	-7.732434000	1.068080000	1.010580000
C	-8.741824000	1.401245000	1.886128000
C	-8.774554000	0.855510000	3.191137000
C	-7.781633000	-0.004378000	3.599426000
C	-5.515092000	0.305892000	-0.886841000
C	-4.425181000	1.084190000	-1.223819000
C	-4.222825000	1.613474000	-2.515107000
C	-5.132595000	1.328075000	-3.503846000
C	-6.254793000	0.498015000	-3.242604000
C	-6.450025000	-0.031671000	-1.922846000
C	-7.182458000	0.167774000	-4.266832000
C	-8.248303000	-0.664516000	-4.015284000
C	-8.427290000	-1.209367000	-2.721816000
C	-7.552828000	-0.902428000	-1.703212000
O	-3.507172000	1.458481000	-0.227373000

O	-3.574318000	-1.402726000	0.158992000
C	-2.417319000	-0.679482000	0.163638000
C	-1.211445000	-1.377362000	0.353434000
C	0.042039000	-0.717431000	0.331375000
C	0.074113000	0.678774000	0.150176000
C	-1.143825000	1.370971000	-0.060833000
C	-2.382278000	0.705126000	-0.057848000
C	-1.291881000	-2.772585000	0.667195000
C	-1.138991000	2.766881000	-0.381630000
N	-1.157769000	3.890471000	-0.679785000
N	-1.384909000	-3.895188000	0.954965000
N	1.217463000	-1.478758000	0.500065000
N	1.279954000	1.410417000	0.167297000
C	2.085288000	-1.448051000	1.607159000
C	3.118455000	-2.394304000	1.397335000
C	2.859141000	-3.021585000	0.119365000
C	1.678699000	-2.453491000	-0.402716000
C	1.624304000	2.373353000	1.134794000
C	2.890787000	2.913484000	0.805538000
C	3.313104000	2.269865000	-0.419517000
C	2.305649000	1.354297000	-0.792284000
C	2.003007000	-0.691770000	2.774452000
C	2.995066000	-0.877483000	3.736148000
C	4.034176000	-1.800978000	3.541948000

C	4.101639000	-2.565241000	2.379930000
C	3.528831000	-4.014740000	-0.619884000
C	2.999411000	-4.417176000	-1.848966000
C	1.819973000	-3.829646000	-2.335685000
C	1.139780000	-2.840830000	-1.633224000
C	0.920999000	2.778281000	2.269188000
C	1.508326000	3.745659000	3.083925000
C	2.764940000	4.289862000	2.776354000
C	3.462087000	3.879982000	1.642563000
C	4.447475000	2.415664000	-1.239839000
C	4.543848000	1.648109000	-2.403104000
C	3.514269000	0.756066000	-2.746918000
C	2.378966000	0.593674000	-1.960927000
H	-5.701396000	-1.627614000	4.160261000
H	-3.826891000	-2.194984000	2.616307000
H	-7.714843000	1.500241000	0.016328000
H	-9.518344000	2.093829000	1.573384000
H	-9.579042000	1.124574000	3.869818000
H	-7.788961000	-0.419611000	4.604294000
H	-3.364675000	2.253694000	-2.691960000
H	-4.999071000	1.734284000	-4.503024000
H	-7.027241000	0.581992000	-5.260099000
H	-8.948335000	-0.912490000	-4.808177000
H	-9.260433000	-1.880306000	-2.531608000

H	-7.696904000	-1.333524000	-0.718831000
H	1.203040000	0.022007000	2.935389000
H	2.958058000	-0.293295000	4.651307000
H	4.791551000	-1.924111000	4.311079000
H	4.891387000	-3.293020000	2.232169000
H	3.486367000	-5.186082000	-2.436182000
H	1.427421000	-4.164617000	-3.291759000
H	0.226217000	-2.405374000	-2.023684000
H	-0.053866000	2.366395000	2.511890000
H	0.978103000	4.082915000	3.970202000
H	3.197347000	5.041354000	3.430934000
H	4.435749000	4.292380000	1.403751000
H	5.406475000	1.733371000	-3.052650000
H	3.612255000	0.174110000	-3.659057000
H	1.597588000	-0.100227000	-2.246078000
O	4.667498000	-4.512319000	-0.060252000
O	5.376673000	3.321719000	-0.821943000
C	6.548615000	3.520674000	-1.615199000
H	6.259362000	3.814529000	-2.634770000
H	7.112158000	2.579175000	-1.678845000
C	7.386615000	4.610146000	-0.959242000
H	8.343768000	4.663192000	-1.497081000
H	7.621432000	4.300318000	0.067879000
C	6.718367000	5.991152000	-0.952908000

H	5.748416000	5.919564000	-0.446911000
H	6.502563000	6.290060000	-1.988700000
C	7.578750000	7.063902000	-0.278483000
H	7.079736000	8.039286000	-0.290685000
H	7.783204000	6.807970000	0.768446000
H	8.545205000	7.177591000	-0.785451000
C	5.389905000	-5.530061000	-0.757022000
H	5.663119000	-5.169167000	-1.757865000
H	4.750367000	-6.415156000	-0.880834000
C	6.626442000	-5.877286000	0.063822000
H	6.293703000	-6.228976000	1.048515000
H	7.118644000	-6.729797000	-0.425370000
C	7.632487000	-4.727520000	0.239307000
H	8.403409000	-5.054187000	0.949318000
H	7.124420000	-3.874928000	0.705443000
C	8.308753000	-4.274664000	-1.059996000
H	9.052838000	-3.495308000	-0.860981000
H	8.824711000	-5.108823000	-1.552508000
H	7.588482000	-3.859437000	-1.774219000

Coordinates for optimized geometry of R-NBTOCZ.

112

symmetry c1

C	7.043451000	1.186649000	1.167757000
C	6.957574000	2.538575000	1.642418000
C	5.870342000	3.355180000	1.233041000
C	4.891835000	2.860842000	0.405571000
C	4.986315000	1.530111000	-0.051861000
C	6.036694000	0.693106000	0.270924000
C	8.113935000	0.375814000	1.636150000
C	9.059568000	0.880128000	2.500965000
C	8.987987000	2.221235000	2.946191000
C	7.956294000	3.028318000	2.526373000
C	6.036731000	-0.693204000	-0.270946000
C	4.986392000	-1.530263000	0.051824000
C	4.891969000	-2.860988000	-0.405636000
C	5.870500000	-3.355268000	-1.233115000
C	6.957699000	-2.538609000	-1.642469000
C	7.043515000	-1.186686000	-1.167782000
C	7.956447000	-3.028294000	-2.526425000
C	8.988110000	-2.221161000	-2.946219000
C	9.059629000	-0.880059000	-2.500971000
C	8.113968000	-0.375799000	-1.636155000
O	4.001178000	-1.088502000	0.949524000

O	4.001119000	1.088280000	-0.949545000
C	2.854648000	0.543969000	-0.441411000
C	1.627658000	1.083262000	-0.879265000
C	0.404344000	0.545692000	-0.437977000
C	0.404380000	-0.546006000	0.438095000
C	1.627721000	-1.083547000	0.879331000
C	2.854679000	-0.544219000	0.441427000
C	1.632392000	2.219762000	-1.748074000
C	1.632518000	-2.220043000	1.748144000
N	1.645691000	-3.154938000	2.439116000
N	1.645508000	3.154656000	-2.439049000
H	5.819390000	4.381169000	1.588056000
H	4.058223000	3.471607000	0.074281000
H	8.175931000	-0.656215000	1.309527000
H	9.866077000	0.240470000	2.848672000
H	9.743072000	2.606656000	3.625578000
H	7.883338000	4.056605000	2.872249000
H	4.058385000	-3.471798000	-0.074361000
H	5.819589000	-4.381250000	-1.588155000
H	7.883537000	-4.056578000	-2.872318000
H	9.743219000	-2.606540000	-3.625605000
H	9.866113000	-0.240360000	-2.848660000
H	8.175919000	0.656227000	-1.309516000
O	-0.759886000	-1.058033000	0.932752000

C	-1.598640000	-1.801187000	0.100558000
C	-1.185556000	-2.349861000	-1.108280000
C	-2.896501000	-2.015267000	0.574364000
C	-2.086830000	-3.119504000	-1.863108000
H	-0.173509000	-2.194934000	-1.465270000
C	-3.623864000	-1.610468000	1.756195000
C	-3.780142000	-2.799718000	-0.213116000
C	-3.387877000	-3.359741000	-1.434719000
H	-1.749084000	-3.543361000	-2.804550000
C	-4.923049000	-2.172665000	1.632240000
C	-3.307695000	-0.840919000	2.882585000
H	-4.064950000	-3.963054000	-2.030257000
C	-5.897226000	-1.985831000	2.617390000
C	-4.278260000	-0.650338000	3.862342000
H	-2.321655000	-0.401011000	2.982024000
C	-5.556568000	-1.218371000	3.729484000
H	-6.886635000	-2.424754000	2.529338000
H	-4.044568000	-0.057552000	4.742151000
H	-6.296348000	-1.060658000	4.509969000
N	-5.006056000	-2.873982000	0.432793000
C	-6.159872000	-3.627788000	-0.029306000
H	-6.172705000	-3.587736000	-1.124456000
H	-7.060991000	-3.103193000	0.308405000
C	-6.179351000	-5.086235000	0.452825000

H	-6.150926000	-5.099062000	1.550440000
H	-5.262233000	-5.585917000	0.113628000
C	-7.408784000	-5.854491000	-0.047555000
H	-7.433600000	-5.827356000	-1.146470000
H	-8.321285000	-5.341976000	0.289566000
C	-7.437165000	-7.310869000	0.427242000
H	-8.325148000	-7.833821000	0.054949000
H	-6.554674000	-7.858989000	0.075978000
H	-7.448893000	-7.370073000	1.522214000
O	-0.759947000	1.057688000	-0.932590000
C	-1.598636000	1.800955000	-0.100442000
C	-1.185537000	2.349615000	1.108398000
C	-2.896461000	2.015158000	-0.574296000
C	-2.086745000	3.119394000	1.863164000
H	-0.173521000	2.194577000	1.465426000
C	-3.623841000	1.610370000	-1.756118000
C	-3.780035000	2.799746000	0.213122000
C	-3.387746000	3.359775000	1.434715000
H	-1.748986000	3.543240000	2.804607000
C	-4.922961000	2.172738000	-1.632239000
C	-3.307740000	0.840689000	-2.882438000
H	-4.064776000	3.963186000	2.030204000
C	-5.897131000	1.985952000	-2.617405000
C	-4.278299000	0.650160000	-3.862210000

H	-2.321754000	0.400646000	-2.981815000
C	-5.556537000	1.218371000	-3.729434000
H	-6.886494000	2.424991000	-2.529411000
H	-4.044654000	0.057279000	-4.741968000
H	-6.296314000	1.060695000	-4.509929000
N	-5.005927000	2.874108000	-0.432818000
C	-6.159607000	3.628205000	0.029158000
H	-6.172618000	3.588088000	1.124304000
H	-7.060814000	3.103878000	-0.308723000
C	-6.178595000	5.086683000	-0.452905000
H	-6.150012000	5.099538000	-1.550517000
H	-5.261372000	5.586074000	-0.113564000
C	-7.407859000	5.855297000	0.047326000
H	-7.432839000	5.828146000	1.146237000
H	-8.320474000	5.343077000	-0.289934000
C	-7.435718000	7.311697000	-0.427442000
H	-8.323588000	7.834920000	-0.055261000
H	-6.553103000	7.859530000	-0.076044000
H	-7.447276000	7.370928000	-1.522415000

References

(1) *Citation | Gaussian.com*. https://gaussian.com/citation/ (accessed 2025-09-28).

(2) Frédéric, L.; Desmarchelier, A.; Favereau, L.; Pieters, G. Designs and Applications of Circularly Polarized Thermally Activated Delayed Fluorescence Molecules. *Adv. Funct. Mater.* **2021**, *31* (20), 2010281. https://doi.org/10.1002/adfm.202010281.

(3) Zhang, D.-W.; Li, M.; Chen, C.-F. Recent Advances in Circularly Polarized Electroluminescence Based on Organic Light-Emitting Diodes. *Chem. Soc. Rev.* **2020**, *49* (5), 1331–1343. https://doi.org/10.1039/C9CS00680J.

(4) Thakur, D.; Vaidyanathan, S. Chiral Lanthanide Complexes in the History of Circularly Polarized Luminescence: A Brief Summary. *J. Mater. Chem. C* **2025**, *13* (19), 9410–9452. https://doi.org/10.1039/D5TC00097A.

(5) Im, Y.; Kim, M.; Cho, Y. J.; Seo, J.-A.; Yook, K. S.; Lee, J. Y. Molecular Design Strategy of Organic Thermally Activated Delayed Fluorescence Emitters. *Chem. Mater.* **2017**, *29* (5), 1946–1963. https://doi.org/10.1021/acs.chemmater.6b05324.

(6) Feuillastre, S.; Pauton, M.; Gao, L.; Desmarchelier, A.; Riives, A. J.; Prim, D.; Tondelier, D.; Geffroy, B.; Muller, G.; Clavier, G.; Pieters, G. Design and Synthesis of New Circularly Polarized Thermally Activated Delayed Fluorescence Emitters. *J. Am. Chem. Soc.* **2016**, *138* (12), 3990–3993. https://doi.org/10.1021/jacs.6b00850.

(7) Wang, T.; Wu, Z.; Sun, W.; Jin, S.; Zhang, X.; Zhou, C.; Jiang, J.; Luo, Y.; Zhang, G. Macroscopic Wires from Fluorophore-Quencher Dyads with Long-Lived Blue Emission. *J. Phys. Chem. A* **2017**, *121* (38), 7183–7190. https://doi.org/10.1021/acs.jpca.7b08268.

(8) Song, F.; Xu, Z.; Zhang, Q.; Zhao, Z.; Zhang, H.; Zhao, W.; Qiu, Z.; Qi, C.; Zhang, H.; Sung, H. H. Y.; Williams, I. D.; Lam, J. W. Y.; Zhao, Z.; Qin, A.; Ma, D.; Tang, B. Z. Highly Efficient Circularly Polarized Electroluminescence from Aggregation-Induced Emission Luminogens with Amplified Chirality and Delayed Fluorescence. *Adv. Funct. Mater.* **2018**, *28* (17), 1800051. https://doi.org/10.1002/adfm.201800051.

(9) Sun, S.; Wang, J.; Chen, L.; Chen, R.; Jin, J.; Chen, C.; Chen, S.; Xie, G.; Zheng, C.; Huang, W. Thermally Activated Delayed Fluorescence Enantiomers for Solution-Processed Circularly Polarized Electroluminescence. *J. Mater. Chem. C* **2019**, *7* (46), 14511–14516. https://doi.org/10.1039/C9TC04941J.

(10) Wu, Z.-G.; Han, H.-B.; Yan, Z.-P.; Luo, X.-F.; Wang, Y.; Zheng, Y.-X.; Zuo, J.-L.; Pan, Y. Chiral Octahydro-Binaphthol Compound-Based Thermally Activated Delayed Fluorescence Materials for Circularly Polarized Electroluminescence with Superior EQE of 32.6% and Extremely Low Efficiency Roll-Off. *Adv. Mater.* **2019**, *31* (28), 1900524. https://doi.org/10.1002/adma.201900524.

(11) Wu, Z.-G.; Yan, Z.-P.; Luo, X.-F.; Yuan, L.; Liang, W.-Q.; Wang, Y.; Zheng, Y.-X.; Zuo, J.-L.; Pan, Y. Non-Doped and Doped Circularly Polarized Organic Light-Emitting Diodes with High Performances Based on Chiral Octahydro-Binaphthyl Delayed

Fluorescent Luminophores. *J. Mater. Chem. C* **2019**, *7* (23), 7045–7052. https://doi.org/10.1039/C9TC01632E.

(12) Liang, Z.-P.; Tang, R.; Qiu, Y.-C.; Wang, Y.; Lu, H.; Wu, Z.-G. Construction and Properties of Octahydrobinaphthol-Based Chiral Luminescent Materials with Large Steric Hindrance. *Acta Chim. Sin.* **2021**, *79*, 1401. https://doi.org/10.6023/A21070355.

(13) Liu, T.-T.; Yan, Z.-P.; Hu, J.-J.; Yuan, L.; Luo, X.-F.; Tu, Z.-L.; Zheng, Y.-X. Chiral Thermally Activated Delayed Fluorescence Emitters-Based Efficient Circularly Polarized Organic Light-Emitting Diodes Featuring Low Efficiency Roll-Off. *ACS Appl. Mater. Interfaces* **2021**, *13* (47), 56413–56419. https://doi.org/10.1021/acsami.1c16223.